

Polarimetric variations of binary stars. IV. Pre-main-sequence spectroscopic binaries located in Taurus, Auriga, and Orion

N. Manset¹ and P. Bastien

Département de Physique, Université de Montréal, C.P. 6128, Succursale Centre-Ville, Montréal, QC, H3C 3J7, Canada, and Observatoire du Mont Mégantic

`manset@cfht.hawaii.edu, bastien@astro.umontreal.ca`

ABSTRACT

We present polarimetric observations of 14 pre-main-sequence (PMS) binaries located in the Taurus, Auriga, and Orion star forming regions. The majority of the average observed polarizations are below 0.5%, and none are above 0.9%. After removal of estimates of the interstellar polarization, about half the binaries have an *intrinsic* polarization above 0.5%, even though most of them do not present other evidences for the presence of circumstellar dust. Various tests reveal that 77% of the PMS binaries have or possibly have a variable polarization. LkCa 3, Par 1540, and Par 2494 present detectable periodic and phase-locked variations. The periodic polarimetric variations are noisier and of a lesser amplitude ($\sim 0.1\%$) than for other types of binaries, such as hot stars. This could be due to stochastic events that produce deviations in the average polarization, a non-favorable geometry (circumbinary envelope), or the nature of the scatterers (dust grains are less efficient polarizers than electrons). Par 1540 is a Weak-line T Tauri Star, but nonetheless has enough dust in its environment to produce detectable levels of polarization and variations. A fourth interesting case is W 134, which displays rapid changes in polarization that could be due to eclipses. We compare the observations with some of our numerical simulations, and also show that an analysis of the periodic polarimetric variations with the Brown, McLean, & Emslie (BME) formalism to find the orbital inclination is for the moment premature: non-periodic events introduce stochastic noise that partially masks the periodic low-amplitude variations and prevents the BME formalism from finding a reasonable estimate of the orbital inclination.

Subject headings: binaries: close — circumstellar matter — methods: observational — stars: pre-main-sequence — techniques: polarimetric

¹Now at: Canada-France-Hawaii Telescope Corporation, 65-1238 Mamalahoa Hwy, Kamuela, HI 96743, USA

1. Introduction

Pre-main-sequence (PMS) stars are objects still contracting to the main sequence (MS) and are divided into 2 classes according to their masses: T Tauri stars (TTS) are low-mass PMS stars with $0.5 M_{\odot} \lesssim M \lesssim 2.0 M_{\odot}$, while Herbig Ae/Be (HAeBe) stars represent their higher-mass counterparts with $2 M_{\odot} \lesssim M \lesssim 10 M_{\odot}$. These 2 classes of objects exhibit properties characteristic of their youth: (1) association with dark or bright nebulosities (remnant of the parent cloud), (2) emission line spectrum (spectral type F or later for the TTS, A or B for the HAeBe), (3) IR excesses, (4) position above the MS in the HR diagram, and (5) presence of the Li I absorption line. Both types of PMS stars show signs of circumstellar (CS) material in their environment, in the form of jets and bipolar flows, emission excesses in the IR, mm and sub-mm domains, P Cygni or inverse P Cygni profiles, linear polarization, and resolved disks or envelopes around some of the objects. In the case of binary stars, the disks can be found around each component (circumstellar (CS) disks) and/or around the binary system (circumbinary (CB) disks). Variability is observed in photometry, spectroscopy, and polarimetry.

TTS are further divided into 2 classes according to the width of their $H\alpha$ emission line. Classical TTS (CTTS) have wide $H\alpha$ emission lines with $W_{\lambda} > 5 \text{ \AA}$ whereas the Weak-line TTS (WTTS) have $W_{\lambda} < 5 \text{ \AA}$ (Bertout 1989). Naked TTS (NTTS) are a subclass of the WTTS (Walter 1986; Wolk & Walter 1996), although some tend to use both terms as synonyms. Indeed, in addition to narrower $H\alpha$ lines, the NTTS specifically do not show evidence for circumstellar (CS) material in their environments in the form of IR excesses, whereas the WTTS may or may not (Wolk & Walter 1996). WTTS and NTTS should not be confused with post-T Tauri stars, which are still above the MS, but more evolved than TTS. For a review on T Tauri stars and Herbig Ae/Be stars, see for example Bertout (1989) and Catala (1989).

Dust grains produce polarization by scattering, polarization that has been known for a number of years (see Bastien 1996 for a review). In general, the red part of the visible spectrum of TTS exhibits linear polarizations of 1–2%, but the polarization distributions of CTTS and WTTS are markedly different: there are a few CTTS which have a very high polarization (more than 5%, sometimes up to 15%), but WTTS almost all have polarization levels below 2% (Bastien 1982, 1985; Ménard & Bastien 1992). Also, most TTS that have an active CS disk have higher polarization and near IR excess than other TTS (Yudin 2000). On average, HAeBe stars are more polarized than TTS (3.0% versus 1.6%), and there are clear differences between the polarization distributions for TTS and HAeBe stars (Yudin 2000). Most PMS stars have statistically higher polarization levels than more evolved stars which are closer to the MS and there is clear evidence of changes in polarimetric behavior of stars during the evolution from PMS to MS star; these changes in polarimetric behavior are related to the evolution of the CS environment (Yudin 2000).

The IR color indices and color excesses of TTS are well correlated with the polarization (Bastien 1985), implying that the same grains are responsible for both phenomena. A compilation of polarization data for almost 500 TTS and HAeBe stars studied by Yudin (2000) reveals that for

85% of the sample stars, there is a correlation between the degree of polarization and the IR color index $(V-L)_{\text{obs}}$ and the color excess $E(V-L)$. This polarization is variable in a majority of objects: more than 85% of the TTS, and more than 70% of HAeBe stars present variability (Bastien 1988; Ménard & Bastien 1992). Variations are sometimes large and fast ($\Delta P > 0.5\%$, $\Delta\theta > 15^\circ$, within 5 days, Bastien 1985), sometimes associated with luminosity and color changes (Grinin et al. 1991; Grinin, Kolotilov, & Rostopchina 1995), and in some cases periodic.

We have shown (Manset & Bastien 2000, 2001a, hereafter Paper I and II) how the linear polarization of a binary surrounded by circumstellar matter varies periodically as a function of the orbital period, and how the geometry of the disks, the nature and characteristics of the scatterers, the masses of the stars, and the orbit characteristics affect the polarimetric curves. Models can be used to find the orbital inclination from observed polarimetric variations (see for example Rudy & Kemp 1978; Brown, McLean, & Emslie 1978). The work from Brown et al. (1978) (hereafter BME) uses first- and second-order Fourier analysis of the Stokes curves to give, in addition to the orbital inclination, moments related to the distribution of the scatterers in the CS and CB environments. The BME formalism was developed for Thomson scattering in optically thin envelopes, and for binaries in circular orbits. Since polarization in PMS stars is produced by scattering on dust grains, and most of the known spectroscopic PMS binaries have eccentric orbits, the BME formalism can not be used a priori. However, we have shown (Paper I and II) that the BME analysis can still be applied in those cases, with a few limitations.

In this context, we have obtained polarimetric observations of 24 spectroscopic PMS binaries. A detailed analysis was presented for one of these binaries, the HAeBe star MWC 1080 (Manset & Bastien 2001b, hereafter Paper III). Here we report the complete observations and detailed analysis for the PMS binaries located in the Taurus, Auriga, and Orion star forming regions (SFRs). Binaries located in the Scorpius and Ophiucus regions will be analyzed in a future paper.

2. Observations

We have observed 24 PMS spectroscopic binaries with $\delta \gtrsim -25^\circ$; the shortest-period and brightest ones ($P \lesssim 35$ d, $V \lesssim 12.0$) were followed with ≈ 10 or more observations. These stars were chosen mainly from the list in Mathieu (1994), to which we added subsequent discoveries. Tables 1 and 2 present basic information (other names, coordinates, location), and spectroscopic and orbital data (spectral type, PMS type, orbital period and eccentricity, orbital inclination when known, and distance) for the 14 binaries located in the Taurus, Orion, and Auriga SFRs.

The binaries were observed at the Observatoire du Mont Mégantic (OMM), Québec, Canada, between 1994 September and 1999 March, using a $8''.2$ aperture hole and a broad red filter (RG645: 7660 Å central wavelength, 2410 Å full width at half maximum). Polarimetric data were taken with Beauty and The Beast, a two-channel photo-electric polarimeter, which uses a Wollaston prism, a Pockels cell, and an additional quarter-wave plate. The data were calibrated for instrumental

efficiency, instrumental polarization (due to the telescope’s mirrors), and zero point of position angle, using a Glan-Thomson prism, non-polarized standard stars, and polarized standard stars respectively. The observational errors were calculated from photon statistics, and also include uncertainties introduced by the previously mentioned calibrations. The final uncertainty on individual measurements of the polarization P is usually in the range 0.03–0.05%. The relative errors in position angle θ can be as low as 0.1° , but due to instrumental effects, systematic errors, and the calibration procedure itself, the absolute errors on the position angles are of the order of 1° . For more details on the instrument and the observational method, see Manset & Bastien (1995, 2001b) and Manset (2000). Table 3 summarizes the observations and gives the number of observations, the average polarization and position angle.

3. Estimation of the interstellar polarization

Polarimetric observations are usually a sum of interstellar (and sometimes also intra-cluster) and intrinsic polarizations. An estimation of the interstellar (IS) polarization for each object observed can be used to assess the presence of intrinsic polarization. We have used the Heiles (2000) catalog of over 9000 polarization measurements to determine if the observed polarization for the PMS binaries studied here is of intrinsic or IS origin, or a combination of both. This catalog is an improvement over the one from Mathewson et al. (1978): it contains additional observations, all data were verified, and more precise coordinates are given.

For each observed PMS binary, the catalog was scanned to select at least 20 close stars *with a similar distance*. Depending on the stellar density and number of measurements in the catalog, this led to the selection of a region between 1 and 15° in radius around the target, and within 70 to 350 pc of it. The stars selected from the catalog are used to give an average of the IS polarization in that region around the target, and also to find the ratio $P/E(B - V)$. Finally, based on an extinction value for our target and assuming this extinction is of IS origin only, an estimate of the IS polarization for the target is calculated, along with the average IS polarization angle. This angle is calculated with a simple average and with a distance-weighted average of the polarization angles of all the stars selected. In all the cases here, the two values are similar to within their uncertainty, which indicates that the alignment is good over all the regions studied, and the IS polarization value estimated is reliable. If the position angles for the IS polarization and for the target are different, it points to an intrinsic origin for at least part of the polarization measured. Intrinsic polarization is also deduced from polarimetric variability.

Results are presented in Table 3, where the weighted averages of the observed P and θ are given along with the possible origin of the observed polarization: a \star symbol indicates intrinsic polarization while IS stands for interstellar polarization. When IS comes before a \star symbol, the IS component of the polarization is probably stronger than the intrinsic one, and vice versa. The following columns present our calculation of the IS polarization (polarization and position angle, along with their uncertainties), based on a weighted average of the polarization of neighboring stars

located at similar distances, where more weight is given to stars closer to the PMS binary. Since non-weighted and weighted averages give similar results, only the latter average is presented. We also give N_{IS} , the number of measurements used to estimate this IS polarization, and the radius and the interval of distance of the region considered. Subtracting the IS polarization from the observed one gives the intrinsic polarization, shown in the last columns.

Note that the IS polarization given in columns 6–9 of Table 3 is only an *estimate* for the *whole region* around a binary, and in some cases might not apply to a given binary. In particular, it may not include very localized intra-cluster polarization. Consequently, the intrinsic polarizations given in the last columns should be considered crude estimations only, intended to give an idea of the polarimetric characteristics of the observed binaries as a whole, and not a definitive value of the intrinsic polarization for each binary.

To determine if an observed polarization has an IS component, we give more weight to the value of θ_{IS} deduced from neighboring stars than to P_{IS} . We do not have the wavelength dependence of the observed polarization, which can usually be used to extract the IS component. To help determine if there is an intrinsic component of polarization, we also use the level of polarimetric variability since IS polarization is very stable.

4. Polarimetric variability

Since a majority of single PMS stars are variable polarimetrically (Bastien 1982; Drissen, Bastien, & St-Louis 1989; Ménard & Bastien 1992), we expected PMS binaries to also be polarimetrically variable, either periodically or not.

4.1. Variability tests

We applied various tests to check the polarimetric variability or stability of PMS binaries: minimum and maximum values, variance test, Z test and a similar one we call σ_1 and σ_2 test, and finally, a χ^2 test. We have not retained skewness and kurtosis tests (which measure departure from a Normal distribution) because the number of data points is for some stars very limited, and the results sometimes difficult to interpret. It should be noted that these tests usually assume that the parent distribution of the quantity measured (here, P , θ , or the Stokes parameters Q and U) is Normal. Since P and θ are not distributed Normally (Serkowski 1958), these tests should in general be applied only to the Stokes parameters Q and U .

Many PMS binaries show observations with polarization levels and/or position angle well below or above the bulk of the data. Assuming these observations are atypical but nonetheless real, we have removed them before using the tests. This allows us to study the more typical variations. We believe these atypical observations are real: close examination of polarization observations

taken over 5 years of non-polarized standard stars (84 observations), polarized standard stars (53 observations), 3 stars that were followed for many consecutive hours (121 observations) did not show odd observations like the ones we repeatedly saw for PMS binaries (Manset 2000). Therefore, we believe these observations were due to some eruption-like events or significant modifications in the CS environment (e.g., formation/destruction of condensations, accretion events), and not because of an instrumental problem.

4.2. Maximum and minimum values

One crude but easy way to check for variability in a set of observations is to compare the difference between the maximum and minimum values of a quantity with its average or typical observational uncertainty; variable observations will have maximum and minimum values well outside the range expected from the observational uncertainty. This test was applied to all the sets of observations, after removing the observations that showed the most deviation from the majority of the observations. This test should not be used alone since it does not take into account the entirety of the data.

4.3. Variance test

Given a set of N observations D_i where $i = 1, \dots, N$, we can calculate the variance of the sample (which is a measure of the “width” of the observations, or of the scatter from the mean, or of the “variability” around a central value, usually measured with the mean \overline{D}) with the formula:

$$\sigma_{\text{sample}}^2 = \frac{1}{N-1} \sum_i (D_i - \overline{D})^2, \quad (1)$$

which, in computer programs, can also be calculated more rapidly (without having first to determine the mean \overline{D}) with:

$$\sigma_{\text{sample}}^2 = \frac{\sum_i D_i^2}{N-1} - \frac{(\sum_i D_i)^2}{N(N-1)}. \quad (2)$$

This sample variance can then be compared to the standard deviation of the mean, which gives the error from photon statistics as if all the observations had been added together:

$$\sigma_{\text{mean}}^2 = \frac{1}{\sum_i 1/\sigma_i^2}. \quad (3)$$

For a set of observations of a non-variable quantity, the sample variance will be low (the observations are all clustered closely to the mean) and similar to the standard deviation of the mean. But if there is variability, the “width” of the observations will be greater than the standard deviation of the mean: $\sigma_{\text{sample}} \geq \sigma_{\text{mean}}$. It should be noted that it is assumed the parent population is distributed Normally, so this test will be meaningful only for the Stokes parameters.

4.4. Z test

Given a quantity D for which we have N measurements $D_i \pm \sigma_i$, we can calculate the weighted mean:

$$\overline{D}_w = \frac{\sum_i (D_i / \sigma_i^2)}{\sum_i (1 / \sigma_i^2)}, \quad (4)$$

with its associated variance, which we will call the “external” variance:

$$\sigma_{w1}^2 = \frac{1}{\sum_i 1 / \sigma_i^2}. \quad (5)$$

Alternatively, the variance may be computed according to the weighted residuals, giving an “internal” assessment of the distribution:

$$\sigma_{w2}^2 = \frac{\sum_i \frac{(D_i - \overline{D}_w)^2}{\sigma_i^2}}{(N - 1) \sum_i 1 / \sigma_i^2}. \quad (6)$$

We then build the quantity Z :

$$Z = \frac{\sigma_{w2}}{\sigma_{w1}} \quad (7)$$

$$= \sqrt{\frac{\sum_i \frac{(D_i - \overline{D}_w)^2}{\sigma_i^2}}{(N - 1)}}. \quad (8)$$

If the data are “well behaved”, Z should equal unity (Brooks et al. 1994).

The standard error of Z is (Topping 1972):

$$\sigma_Z = \frac{1}{2(N - 1)}. \quad (9)$$

This test should be applied to Q and U , and not to P and θ . If $Z \approx 1$ within its standard error, then the measurements are “consistent”, and there is no variability. If Z differs significantly from 1, then there may be variability. For details, see Brooks et al. (1994).

4.5. σ_1 and σ_2 test

The σ_1 and σ_2 test is similar to the Z test, except that it is applied to the polarization P and its position angle θ . Given a set of N polarimetric observations of the Stokes parameters Q and U , we can compare the variance of the polarization $\sigma_1^2(P)$ with the scatter from the mean of the polarization $\sigma_2^2(P)$:

$$\sigma_1^2(P) = N \left[\sum_i \frac{1}{\sigma_i^2} \right]^{-1}, \quad (10)$$

$$\sigma_2^2(P) = \frac{\sum_i (Q_i - \bar{Q})^2 + \sum_i (U_i - \bar{U})^2}{2(N-1)}. \quad (11)$$

For the position angle, we can calculate $\sigma_1(\theta)$ and $\sigma_2(\theta)$ with the following formula:

$$\sigma(\theta) = 28.65 \frac{\sigma(P)}{P}. \quad (12)$$

If $\sigma_2 > \sigma_1$ then there may be variability. Bastien et al. (1988) used this method to assess the polarimetric variability of polarimetric standard stars. Clarke & Naghizadeh-Khouei (1994) make the remark that σ_2 should be the weighted mean.

4.6. χ^2 test

In Bastien et al. (1988) and Bastien (1982), a χ^2 -based method is presented: χ^2 values are calculated for Q and U separately, using $1\sigma_i$ and $1.5\sigma_i$. Then, the probability to obtain a given value of χ^2 in a Gaussian distribution is found for each of the four χ^2 values. The star is variable if at least 2 of the four χ^2 values are over 0.95; the star is suspected to be variable if one out of four χ^2 values is over 0.95.

4.7. How to use the variability tests

The minimum and maximum values test is not a robust test; stars that do not show minimum and maximum values out of the range expected from the observational uncertainty ($\pm 1\sigma$ intervals) are found to have a non-variable behavior by other tests, but the converse is not true.

The variance and Z tests were used only for the Stokes parameters (and not for the polarization and its position angle). The Z test was considered positive if $Z > 1.0 + \sigma_Z$; values of Z below $(1.0 - \sigma_Z)$ were considered dubious, since $Z < 1.0$ means the data are too well behaved with respect to the statistical (observational) uncertainty. The variance test was considered positive if $\sigma_{\text{sample}} \geq 3.0 \sigma_{\text{mean}}$; that way, the variance and Z tests would give consistent results. With $\sigma_{\text{sample}} \geq \sigma_{\text{mean}}$, the variance test would sometimes see variability where the Z test would not.

The σ_1 and σ_2 tests were not considered as primary tests, since they apply to P and θ , which are not Normally distributed, and because σ_2 is not weighted. But the results of this test agree with the conclusions reached with other tests.

For the χ^2 test, as in Bastien et al. (1988) and Bastien (1982), the star is considered variable if at least 2 of the four χ^2 values are over 0.95; the star is suspected to be variable if one out of four χ^2 values is over 0.95.

Using, for Q and U separately, the $\sigma_{\text{sample}} \geq 3.0 \sigma_{\text{mean}}$ test, the $Z > 1.0 + \sigma_Z$ test, and the χ^2

test, we established the variability, suspected variability, suspected stability, and stability with the following criteria (see also Table 4):

- To be considered variable, a star must have at least 2 positive results from the Z and variance tests and at least 2 positive results from the χ^2 test;
 - if there are only 2 positive results from the Z and variance tests, they must be 2 positive Z tests, or a positive Z and positive variance tests for the same Stokes parameter;
 - if there are only 2 positive results from the χ^2 test, they must be for the same Stokes parameters as the positive Z and variance tests.
- To be considered as suspected variable, the results of the Z and variance tests must be the same as for the variable conclusion, but only one χ^2 value must be positive.
- A star is considered as possibly constant if the χ^2 test is negative (for the 4 χ^2 values), but at least 3 values from the Z and variance tests indicate possible variability.
- If the Z and χ^2 tests are negative and only 1 or 2 values of the variance test indicate variability, the star is considered to be constant.

4.8. Results of variability tests for the PMS binaries

Table 5 presents the amplitude of the polarimetric variations, calculated by simply taking the difference between the minimum and maximum values of P , θ , Q and U ; note that for some cases, very atypical observations were not considered. The details of the variability tests presented in this sections are shown in Table 6, where we give for each star the number of observations used for the variability tests, σ_{sample} and σ_{mean} , Z and its standard error, and $P\chi^2$, calculated with 1σ and 1.5σ . The conclusions of the variability tests are shown in Table 7, where we have classified the stars as “variable”, “suspected variable”, and “constant”. Of the 12 binaries which were tested for variability, 42% (5/12) are statistically variable (V773 Tau, V826 Tau, GW Ori, Par 1540, W 134), and 58% (7/12) are variable or possibly variable (Par 2486, Ori 569). DQ Tau and UZ Tau E/W could not be tested because of the low number of observations ($N = 1$ and $N = 2$ respectively). Five binaries have statistically constant polarization: LkCa 3, NTTS 045251+3016, Ori 429, Par 2494, and VSB 126. We confirm the variability already reported for V773 Tau (Ménard & Bastien 1992). Our additional data establish the variability for the previously suspected variables V826 Tau (Ménard & Bastien 1992) and GW Ori (Bastien 1985).

5. Periodic polarimetric variations

In addition to the general variability, which is a known property of single PMS stars, PMS binaries will also present periodic polarimetric variations caused by the orbital motion, even if in

some cases the amplitude may be too small to be detected with the currently available instruments or masked by non-periodic or pseudo-periodic variations. In the case of Mie scattering, we have also shown in Paper II that dust grains, which are mostly responsible for the polarization here, are less efficient polarizers and produce smaller amplitude variations than electrons. This is an indication that periodic polarimetric variations could be more difficult to observe in PMS binaries than in, for example, hot binaries surrounded by electrons, which can easily exhibit variations of a few tenths of a percent (see for example Robert et al. 1990; Robert et al. 1992). The size of the grains also determines the amplitude of the polarimetric variations: dust grains with radii $\sim 0.1\mu\text{m}$ produce the largest polarimetric variations (Paper II).

To look for periodic polarimetric variations, the known orbital periods are used to calculate the orbital phase for each observation of each star. The polarization P , its position angle θ , and the Stokes parameters Q and U are plotted as a function of the orbital phase (see Figures 2 to 20). When enough data are available, observations are represented as first and second harmonics of $\lambda = 2\pi\phi$, where ϕ is the orbital phase:

$$Q = q_0 + q_1 \cos \lambda + q_2 \sin \lambda + q_3 \cos 2\lambda + q_4 \sin 2\lambda, \quad (13)$$

$$U = u_0 + u_1 \cos \lambda + u_2 \sin \lambda + u_3 \cos 2\lambda + u_4 \sin 2\lambda. \quad (14)$$

The coefficients of this fit are then used to find the orbital inclination, following the BME formalism and using the first or second order Fourier coefficients, although it is usually expected that second order variations will dominate (BME):

$$\left[\frac{1 - \cos i}{1 + \cos i} \right]^2 = \frac{(u_1 + q_2)^2 + (u_2 - q_1)^2}{(u_2 + q_1)^2 + (u_1 - q_2)^2}, \quad (15)$$

$$\left[\frac{1 - \cos i}{1 + \cos i} \right]^4 = \frac{(u_3 + q_4)^2 + (u_4 - q_3)^2}{(u_4 + q_3)^2 + (u_3 - q_4)^2}. \quad (16)$$

As can be seen in Figures 2 to 20, not all PMS binaries show periodic polarimetric variations, and even then, those are not always clearly seen, which was expected to some extent. Periodic polarimetric variations can be caused by the binarity (orbital motion) or the presence of hot or cool stellar spots, among a few reasons. Classical T Tauri Stars (CTTS) are known to have both cool and hot spots, and WTTS generally have only cool spots (Bouvier et al. 1993), some of which can be stable over periods of several months (on V410 Tau for example, Herbst 1989). Since most of the binaries observed here are WTTS and in general only display small photometric variations, we believe that the spots causing the photometric variations, if present, are small, and then have a very small effect on the polarization. Nonetheless, as can be seen in the figures, the appearance and disappearance of transient spots could be the cause of the non-periodic variations that introduce some scatter about the periodic variations. In addition to stellar spots, non-periodic phenomenon such as eruptive events, variable accretion and rearrangements of the CS or CB material can cause

pseudo-periodic polarimetric variations that may mask the strictly periodic ones, especially if the observations are taken over many orbital periods, as is the case here.

Despite these difficulties, some binaries present periodic variations. To investigate the significance of this periodicity, a Phase Dispersion Method (Stellingwerf 1978) and a Lomb normalized periodogram algorithm (Press et al. 1997) were used. The Phase Dispersion Method (PDM) is a least-squared fitting technique suited for non-sinusoidal time variations covered by irregularly spaced observations, and finds the period that produces the least scatter about the mean curve. The Lomb normalized periodogram (LNP) method is more powerful than Fast Fourier Transform methods for uneven sampling, but still assumes the curve is sinusoidal, which may not be always appropriate for the polarimetric observations presented here. The periods found by using both methods are very similar to one another for a given star, but the significance is usually marginal.

6. Comments on individual stars

The detailed observations are presented in Tables 8 to 18 and in Figures 2 to 20.

6.1. V773 Tau = HBC 367 = HD 283446

V773 Tau is a triple system in which the 51.075-day spectroscopic binary (Welty 1995) has a projected separation of 0.34 AU (Jensen & Mathieu 1997). The third star is reported to be at $0''.17$ from the spectroscopic binary at a position angle of 295° (Leinert et al. 1993), or $0''.112$ at position angle 295° (Ghez, Neugebauer, & Matthews 1993). Given the size of our aperture hole, this third star is also included in our measurements. Jensen, Mathieu, & Fuller (1994) report for the tertiary a projected separation of 16 AU. The IR excess of $K - N = 3.4$ mag indicates the presence of an optically thick inner disk at $10 \mu\text{m}$ (Simon & Prato 1995). No CB disk was detected at 2.7 mm by Dutrey et al. (1996), but Jensen & Mathieu (1997) argue that the submm continuum emission must arise in a CB disk, although the presence of a third star could mean the submm and IR excesses are not coming from a CB disk, but from a CS disk around the tertiary. The 3σ upper limit to the disk’s mass, based on $800 \mu\text{m}$ observations, is $0.001 M_\odot$ (Jensen et al. 1994). V773 Tau is highly variable in the mm, submm, and radio domains (Jensen et al. 1994; Dutrey et al. 1996), but simultaneous observations in the radio, optical, and X-ray regions by Feigelson et al. (1994) showed variations only in the radio.

From the polarization catalog of Heiles (2000), we find a very low IS polarization in the vicinity of V773 Tau, $0.07\% \pm 0.08\%$ at a position angle $72^\circ \pm 36^\circ$ (see Table 3). This value was found by averaging the polarization of 24 stars located within 15° and 85 pc of V773 Tau. A map of the IS polarization in the vicinity of V773 Tau is presented in Figure 1, where it is seen that the polarization of neighboring stars is low. V773 Tau’s polarization is significantly higher than the IS estimate, and is variable (see below), pointing to intrinsic polarization. We conclude that

V773 Tau’s polarization is intrinsic with maybe a small IS component.

Data are presented in Table 8 and Figure 2. V773 Tau’s mean polarization at 7660 Å is 0.35% at 88°. This position angle is not correlated with the position angle of the third star². V773 Tau was observed in polarimetry by Bastien (1982, 1985) and Ménard & Bastien (1992). Combined with the new data, the earlier observations (taken in red filters, centered on ≈ 7600 Å, and having widths of ≈ 800 Å for the data of Bastien (1982) and Ménard & Bastien (1992), and 2410 Å for our data) reveal that the polarization and especially its position angle are variable on a time scale of a decade: the polarization was 0.10% at 72° in fall 1978, 0.33% at 108° in winter 1985, and 0.35% at 88° in 1999. There are also large variations as a function of wavelength.

Using all data available at the time, Ménard & Bastien (1992) found V773 Tau to be variable at least in position angle, in the blue and green parts of the optical spectrum. We confirm that P and θ are variable, in the red spectral domain. This variability is a strong indication that part of the polarization is intrinsic, in agreement with the presence of some material as indicated by the IR and mm observations and with our analysis of the IS polarization in this region. Our variability analysis is based on 6 observations, one of which presents a polarization ($P \approx 0.2\%$) well below the average of the 5 other observations ($P \approx 0.4\%$), although its position angle agrees well with the other observations. This low polarization observation was the first observation taken, and it was taken a year before the next one. This might indicate a change in the environment of this triple system over the course of one year. All the polarimetric data available present evidence for long-term (decades, years) and short-term (months) variability, as well as variability as a function of wavelength. The limited number of observations (6) does not permit us to find any periodic polarimetric variations or to do a fit according to equations 13 and 14.

Since the third star in this system (included in our aperture hole) is faint (brightness ratio at K of 0.13; Leinert et al. 1993), most of the polarization comes from the spectroscopic binary. As mentioned before, the submm emission could come from a CS disk around the tertiary instead of a CB disk around the spectroscopic binary, but such a geometry would probably not produce the polarimetric variations observed over a few months.

6.2. LkCa 3 = HBC 368

LkCa 3 is a triple system (Simon & Prato 1995) in which the 12.941-day period secondary (Mathieu 1994) is 0.47" from the primary (Dutrey et al. 1996), at a position angle of 78° (Leinert et al. 1993; Ghez et al. 1993). In a series of 26 BVR photometric observations, Grankin (1993) found photometric variations of the order of 0.7 mag in V , but no period could be found. The low excess $K - N = 0.1$ mag indicates that there might be an optically thin inner disk at 10 μm or no

²Since position angles on the sky are measured from 0° to 360° but polarization position angles only from 0° to 180° the 295° position angle for the third star would give a polarization position angle of 65°.

disk at all (Simon & Prato 1995). Wolk & Walter (1996) attribute the IR flux to the photosphere, and not to optically thin material. No CB disk was detected at 2.7 mm (Dutrey et al. 1996).

LkCa 3 is within half a degree of V773 Tau, in a similar region of low polarization (see Table 3 and Figure 1). Most if not all of the low polarization observed for LkCa 3 could therefore be of IS origin, which agrees with the fact that there is little or no indication of CS or CB material. Data are presented in Table 9 and in Figure 3. LkCa 3’s average polarization, 0.05% at 76° , has a position angle close to the position angle of the secondary (78°). Statistically, the polarization is constant, which agrees with its predominant IS origin. However, there are some periodic behavior in the position angle: between phases 0.2 and 0.65, the variations outline a sinusoidal wave (see Figure 3). Statistical tests that check for variability do not taken into account such systematic, although small, variations, and low-level variability may not be completely ruled out.

6.3. V826 Tau = HBC 400 = TAP 43

The projected separation between the two components of this 3.88776-day binary (Mathieu 1994) is 0.06 AU (Jensen et al. 1994). Although this WTTS is a PMS star with an estimated age of 10^6 yr (Mathieu, Walter, & Myers 1989), it is a mature system, with a circular orbit and no evidence for circumstellar material. It shows weak $H\alpha$ emission lines superimposed on a normal continuum, UV excess, and strong X-ray emission, but lies above the MS (see Mundt et al. (1983), who review the multiple evidences for the youth but evolved status of this star). The weak $H\alpha$ emission and absence of veiling (Lee, Martin, & Mathieu 1994) suggest a small or nil accretion rate. Rydgren & Vrba (1983a) did not detect IR excess, whereas Weaver & Jones (1992) possibly did, indicating that there might still be some material in the environment; Wolk & Walter (1996) attribute the IR flux to the photosphere, and not to optically thin material. There is no evidence for an associated disk, mass accretion or mass loss (Mathieu et al. 1989). No CB disk was detected at 2.7 mm (Dutrey et al. 1996). V826 Tau was not detected at $1100\ \mu\text{m}$ (Skinner, Brown, & Walter 1991), so an upper limit to the disk mass based on the 3σ upper value of the $1100\ \mu\text{m}$ observations gives an upper 3σ limit of $0.03\ M_\odot$. The 3σ upper limit to the disk’s mass, based on $800\ \mu\text{m}$ observations, is $0.007\ M_\odot$ (Jensen et al. 1994).

This star also has a photometric period (Rydgren & Vrba 1983b) of 4.05 ± 0.2 d. The photometric minima is shifting with time, possibly due to changes in the spot numbers or position (Reipurth et al. 1990). Stellar spots could introduce polarimetric variations through non-uniform illumination of the CS material; these variations would then have a period of ≈ 2.0 d, half of the photometric period. Mundt et al. (1983) have deduced from spectroscopic observations an orbital inclination of 7.2° , compatible with the inclination of 13° found by Reipurth et al. (1990), a circular orbit and mass ratio of 1.0, which has been confirmed by Reipurth et al. (1990) and Lee et al. (1994). This mass ratio and circular orbit simplify the interpretation of the polarimetric variations based on our numerical simulations (Papers I and II). With such a low inclination, our numerical models predict variability in position angle ($\Delta\theta \approx 15^\circ$), but not in polarization.

Our polarimetric data for V826 Tau are presented in Table 10 and Figure 4, where the fit made according to equations 13 and 14 is also presented. Since the IS polarization is very low in the vicinity of V826 Tau, $0.04\% \pm 0.05\%$ (see Table 3 and Figure 5), the observed polarization, 0.85% at 67° , is probably almost entirely intrinsic, despite the fact that there is no indication for large amounts of CS material.

Ménard & Bastien (1992) presented polarimetry of V826 Tau obtained with a 4700 \AA filter and concluded that the star was possibly variable. We note that P and θ are very similar in the blue (data from 1984, Ménard & Bastien 1992) and in the red (this paper), although the observations were taken years apart. Our statistical tests conclude that the star is variable, but neither set of data clearly shows periodic variations. In particular, we do not see the variability in position angle that would indicate a low orbital inclination, but there is a variability in polarization level, although it is not clear that it is periodic (see Figure 4). To see if spots could be responsible for the polarimetric variations, half of the photometric period was used instead of the orbital one, but this does not reveal any clearer periodic variations. The intrinsic polarization and polarimetric variability are puzzling in regard of the lack of evidence for CS material. This indicates that polarimetry might be more sensitive to the presence of dust than other techniques.

6.4. UZ Tau E/W = HBC 52

UZ Tau is a quadruple system; the E and W binaries are $3''.78$ apart (530 AU with an assumed distance of 140 pc), at a position angle of 273° (Leinert et al. 1993). Our measurements, made with an $8''.2$ aperture hole, include the east and west components, although the brighter E component contributes more to the measurements. The west component, UZ Tau W, is a close binary (Simon & Prato 1995) with a separation of $\sim 0''.35$ (50 AU), at $\sim 0^\circ$ position angle (Leinert et al. 1993; Ghez et al. 1993). It is not surrounded by a CB disk, and has less material ($0.002\text{--}0.04 M_\odot$) than the east component (Jensen, Koerner, & Mathieu 1996b). According to Simon & Prato (1995), both binaries have $K - N$ values that indicate optically thick inner disk regions in the IR: UZ Tau E has $K - N = 2.3$ mag and the W component has $K - N = 2.8$ mag.

UZ Tau E is a single-lined spectroscopic binary, with a projected primary semi-major axis of 0.03 AU (Mathieu, Martin, & Maguzzu 1996); its position angle measured eastward from north is $33 \pm 14^\circ$ (Dutrey et al. 1996). Although no CB disk was detected at 2.7 mm (Dutrey et al. 1996), Jensen & Mathieu (1997) argue that the submm continuum emission must arise in a CB disk. This disk shows no evidence for central clearing, has a mass of $0.06 M_\odot$ and a radius of 145 AU (Jensen et al. 1996b), and is a reservoir of material for active accretion (Mathieu et al. 1996). The SED is well reproduced by a continuous accreting disk, although the SED and emission feature at $10 \mu\text{m}$ can also be fit with a partially evacuated hole (Jensen & Mathieu 1997). Being a close spectroscopic binary does not remove much material, as opposed to wider binaries like the W component (Jensen et al. 1996b).

The structure around UZ Tau E has a FWHM of 300 AU, and is oriented at position angle 19° , compatible with the orientation of the binary ($33 \pm 14^\circ$, Dutrey et al. 1996), previous polarization measurements (Jensen, Mathieu, & Fuller 1996a), and our first measurement (see Table 18). The fact that the position angles of the disk and polarization are similar indicates that most of the polarization is intrinsic (otherwise, if it were interstellar, the polarization angle would not be related to the position angle of the disk), or that the IS polarization angle is the same as the physical elongation of the circumbinary disk. The CO emission has a 2:1 aspect ratio, which suggests that the system is seen more edge-on than pole-on (Jensen et al. 1996b), which is in agreement with the flattening of the radio continuum emission and indicates an orbital inclination of about 70° (Dutrey et al. 1996).

Our 2 measurements, taken a few months apart, are presented in Table 18. Polarimetric observations were also made by Bastien (1982, 1985). Bastien (1982) presented two measurements made in the fall 1977, one with a red filter, narrower than ours, and with a bigger aperture hole of $10''.1$. The polarization was 0.45% at $2^\circ.4$, whereas we measured an average of 0.8% at 16° ; the polarization was then significantly lower in the past but the position angle could be similar. Two measurements made with a green filter (5895Å) in the fall 1977 (Bastien 1982) and winter 1980 (Bastien 1985), and with similar aperture holes ($10''.1$ and $12''.6$) are statistically different: 0.47% at $9^\circ.2$ and 1.02% at $13^\circ.7$. Our 2 observations are also statistically different, showing a change of 0.5% and 45° in 4 months. All the available data indicate that there is some variability on time scales of months and years, and that part of UZ Tau’s polarization is intrinsic. The significant change in polarization angle possibly indicates modifications of the CS and CB environments of this quadruple system.

The IS polarization in a region 15° and ± 70 pc around UZ Tau E/W is very low, $0.11\% \pm 0.05\%$ (see Table 3 and Figure 1) pointing to an intrinsic origin for this binary’s polarization, with maybe a small IS component. The long term variability exposed earlier is compatible with this conclusion.

6.5. DQ Tau = HBC 72

Simon & Prato (1995) report $K - N = 3.5$ mag for both stars of this 15.8-day binary (Stassun et al. 1996), which indicates the presence of an optically thick inner disk. Stassun et al. (1996) give a larger NIR excess ($K - N = 4.2$ mag) which, with the emission observed in the mm, indicates the presence of a massive CB disk, as has also been found by Jensen & Mathieu (1997) from submm continuum emission. The SED gives no indication of an inner hole or gap (Mathieu et al. 1997), but the data could still be consistent with a small amount of residual warm material in a central hole. The CB disk would have a mass of 0.002–0.02 M_\odot (Mathieu et al. 1997).

The mass ratio is indistinguishable from unity. Each star is 3×10^6 yr old and has a mass of 0.65 M_\odot . With an adopted total mass of 1.3 M_\odot , the inclination is 22° (Mathieu et al. 1997).

There could be a third star in this system: there is a faint star $7''.3$ from the binary, at position angle $\sim 150^\circ$; alternatively, it could be a reddened background star (Mathieu et al. 1997). There are recurring flare-like events with the same period as the orbital one, and these occur just before periastron passage, at least 65% of the time. With an eccentricity of $e = 0.556$, the periastron separation is 0.060 AU or 13 stellar radii. The flares are caused by variable accretion (Mathieu et al. 1997). It could be very interesting to monitor the polarization variations during periastron passages.

DQ Tau was observed by Breger (1974), who measured $1.1 \pm 0.3\%$ at 46° , without any filter. Our single observation (see Table 18) is 0.6% at 79° . DQ Tau is located in the same area as V826 Tau, where the IS polarization is low (see Table 3 and Figure 5), but could contribute to DQ Tau’s polarization.

6.6. NTTS 045251+3016 = HBC 427 = TAP 57

NTTS 045251+3016 is a long-period spectroscopic binary with a period of over 2500 d (Mathieu 1994); its projected separation is 4.0 AU (Jensen et al. 1994). The IR excess is $K - N = 0.6 \pm 0.2$ (Simon & Prato 1995) which might indicate that there is an optically thin inner disk or no disk at all; Wolk & Walter (1996) conclude that the minimal excess seen in K and L could be attributed to cool spots or to the companion, and not necessarily to optically thin material. NTTS 045251+3016 was not detected at $1100 \mu\text{m}$ (Skinner et al. 1991), so an upper limit to the disk mass based on the 3σ upper value of the $1100 \mu\text{m}$ observations is $0.02 M_\odot$. In a series of 26 BVR photometric observations obtained during August and September 1992, Grankin (1993) found variations of the order of 0.15 mag in V , but no period could be found. According to Zakirov, Azimov, & Grankin (1993), brightness variations in V had an amplitude of 0.25 mag in 1991/1992, with a rotational period of 9.32 d; no eclipsing effect could be found.

NTTS 045251+3016’s low polarization (0.1% at 107° - see Table 18) may be entirely IS, which would be compatible with the lack of evidence for CS material. However, its position angle is different than the one for the IS polarization, $58 \pm 9^\circ$ (see Table 3 and Figure 6), pointing to an intrinsic origin for part of the polarization. The polarization was determined to be statistically constant, although the long period has not been sampled adequately to reveal orbital variations in the polarization.

6.7. GW Ori = HBC 85 = HD 244138

GW Ori was discovered by Mathieu et al. (1991) to be a spectroscopic binary with a period of 241.9 days, a separation ~ 1 AU and an eccentricity almost indistinguishable from zero. The center-of-mass velocity implies a third star with an orbital period of many years or a $m = 1$ perturbation on the disk (Mathieu et al. 1991). It is one of the brightest CTTS. Based on evolutionary tracks,

the primary is massive ($2.5 M_{\odot}$, Mathieu et al. 1991), and young (1×10^6 yr).

There are large NIR and FIR excesses, with a strong silicate emission feature, and a dip between 2 and 20 μm that could be due to a gap from 0.17 to 3.3 AU in the optically thick disk, gap where the secondary would then be located (Mathieu et al. 1991). Mathieu et al. (1991) have considered two models to reproduce the flat SED; the first one is composed of a circumprimary and a circumbinary disks, and optically thin dust in the gap between these two disks; the second one is composed of a circumbinary shell of inner radius 100 AU with a circumbinary disk. Submillimeter observations are inconsistent with the disk-envelope model (Mathieu et al. 1993), but indicate GW Ori is surrounded by a massive 500 AU circumbinary disk with a model-independent lower mass of $0.3 M_{\odot}$ (with a range from 0.07 to $0.8 M_{\odot}$), with an uncertainty of a factor of 3 due to opacity normalization. The strong $\text{H}\alpha$ emission suggests accretion, but on the other hand, there is no veiling (Schneeberger, Worden, & Wilkerson 1979; Basri & Batalha 1990). A single steady-accretion disk can not reproduce the SED, and a more luminous CB disk is required (Mathieu et al. 1995). Mathieu et al. (1995) study again pure-disk and disk-shell models. The pure-disk model gives a disk mass of $1.5 M_{\odot}$, within a factor of three, which is a significant fraction of the total stellar mass. The disk-shell model falls short of reproducing the submillimeter observations. The large submillimeter emission detected within 500 AU of the binary is not due to the inner part of a more extended infalling envelope, but such an envelope could be responsible for the FIR emission.

A high-resolution interferometric map obtained at 1360 μm reveals a source size of $1''.7 \times 0''.8$ at position angle 56° , although this result must be considered with caution since the source size is smaller than the beam size (Mathieu et al. 1995); this angle is not related with the polarization position angle which we found to be between 115° and 130° (see Table 11).

The inclination is reported to be $15 \pm 1^\circ$ by Bouvier & Bertout (1989) although this value is very uncertain. Mathieu et al. (1991) argue that if a substantial fraction of the total luminosity of this system is due to CS material, then this inclination of 15° is a lower value, and in fact they found 27° . On the other hand, Shevchenko et al. (1992) found Algol-like fadings of 0.4 mag in V due to CS material around the secondary star and near phase 0.0, which would imply an orbital inclination between 80° and 90° .

In 1984 February, Bouvier and Bertout monitored this star to investigate the presence of periodic photometric variations that could be explained by the presence of hot or cool spots. The variations observed seem periodic with a period of 3.2 days, but are of very low amplitude, the highest amplitude being for the U filter, with an amplitude of ~ 0.1 mag. The simple one-spot model could not be satisfactorily applied to the observations.

The average IS polarization, found by averaging the polarization of 30 stars within 10° and 200 pc of GW Ori, is very low in the vicinity of GW Ori, $0.04\% \pm 0.04\%$ (see Table 3) but the IS polarization map (see Figure 7) shows some polarized stars with aligned vectors. We conclude that its polarization is mostly intrinsic with maybe an IS component, which is compatible with the presence of variability (see below). Table 11 and Figure 8 present polarimetric data obtained

over a little more than 3 orbits, along with the fit made according to equations 13 and 14. The data are clearly variable, but not periodically. GW Ori was also observed in polarimetry by Hough et al. (1981), Bastien (1982, 1985) and Ménard & Bastien (1992). Data taken in the winter 1976 (Bastien 1982) and winter 1980 (Bastien 1985) with the same 5895 Å filter show a drastic difference that could be intrinsic or due to the different aperture holes used (14''3 and 4''3): 0.21% at 103° and 2.64% at 151°. If we compare our observations taken between 1996 and 1999 with an earlier observation made with a red but narrower filter, and a bigger aperture hole of 14''3 in winter 1976, we note again a difference: 0.35% at 102° versus 0.61% at 126° on average. There is also a significant rotation of the position angle as a function of time and wavelength (151° at 5895 Å in 1980 (Bastien 1985), 95° at 4700 Å in 1984 (Ménard & Bastien 1992), 126° at 7660 Å, this work). Ménard & Bastien (1992) classified GW Ori as a suspected variable; the data presented here clearly indicate variability. In summary, GW Ori’s polarization and position angle are variable as a function of wavelength and time, on time scales of months and years. As mentioned above, this is an indication in favor of intrinsic polarization, although there also may be a component of IS polarization.

The fact that it shows variability but no clear periodic variations may be an indication that important changes in the circumstellar environment occur over one orbit, or that the star is active. Since the presence of a massive CB disk is inferred from the spectral energy distribution, such changes could be possible.

If this binary has a high inclination as claimed by Shevchenko et al. (1992), rapid changes in the polarization should be observable near phase 0.0, but our sampling is not sufficient near that phase. On the other hand, there could be an important variation in the polarization angle between phases 0.7 and 0.9 (see Figure 8).

6.8. Par 1540 = HBC 447 = NGC 1977 334

This 33.73-day binary (Mathieu 1994) does not present photometric variations over 0.5 mag in *V*; there is no evidence for a significant IR excess; both components are NTTS (Marshall & Mathieu 1988). The mass ratio is 1.32 ± 0.03 ; the weak H α emission and absence of veiling indicate small or nil accretion rate (Lee et al. 1994). Of the five double-lined PMS binaries studied by Lee (1992) (V826 Tau, Par 1540, Ori 429, Ori 569, and NTTS 162814-2427), Par 1540 has the lowest age, 10^5 yr, and the highest Li I abundance.

The polarization for Par 1540, 0.83% at 77° in the 7660 Å filter (see Table 3), is mostly of intrinsic or at least local (intra-cluster) origin, with a smaller IS component. The polarization of nearby stars is low and $\approx 0.30\% \pm 0.05\%$ at 64° (see the map in Breger 1976, our estimation of the IS polarization in Table 3, and a map of IS polarization in Figure 9). Par 1540’s extinction is $E(B - V) = 0.35$ (Marshall & Mathieu 1988), while the reddening between Earth and the Orion Nebula is only $E(B - V) = 0.05$ (Breger, Gehrz, & Hackwell 1981). The polarimetric variability

(see below) also indicates the presence of intrinsic polarization. Par 1540’s position angle is 77° , typical of the less polarized stars studied by Breger (1976), and similar to the average (64°) of stars within its neighborhood and with similar distance. This indicates the presence of an IS polarization component.

Our data are presented in Table 12, Figures 10 and 11. Breger (1976) measured a polarization of $1.11 \pm 0.10\%$ at 85° , without any filter (giving an effective wavelength between B and V). This value is above the average of our measurements, but this could be due to the wavelength dependence of the polarization. Data obtained with the polarimeter STERENN at the Pic-du-Midi Observatory (France) with a V filter and a 10° aperture hole on 14 January 1994 gives a polarization of $0.992 \pm 0.129\%$ at 83° (F. Ménard 2001, private communication), very similar to Breger’s measurement and possibly indicating long-term stability, although our data is clearly variable, in polarization and position angle, on time scales of months and years.

In Figure 10, one atypical point is not shown; many binary PMS stars, like Par 1540, showed atypical values of the polarization that were removed from the data set before fitting the data. Nonetheless, the data is very noisy, and hard to fit according to equations 13 and 14. Statistical tests conclude that the polarization is variable. In Figure 11, the data were binned by dividing the phase into 10 bins and averaging all the polarization observations in each bin. This makes small amplitude periodic variations stand out more clearly, and the quality of the fit is increased. The LNP shows two peaks at 21.3 and 16.2 d, with only slightly better than 50% chance of not being a signature of random Gaussian noise; the former period is also found by the PDM while the latter could reflect the double-periodic low amplitude variations that appear in the binned data (see Figure 11).

6.9. Par 2486 = NGC 1977 1060 = BD −05 1340

The mean polarization of that 5.1882-day binary (Mathieu 1994), 0.14% at 63° (see Table 13 and Figure 12), is mostly IS with also an intrinsic component. Located near Par 1540 (see map in Figure 9), it is in a region of low IS polarization. The average IS position angle is 73° , close to the observed one. Statistical tests indicate possible variability in polarization and position angle, on time scales of months and years. More polarimetric observations would help confirm the variability

6.10. Ori 429 = ORINTT 429

This 7.46-day binary (Mathieu 1994) has a mass ratio is 1.01 ± 0.07 . The weak $H\alpha$ emission and absence of veiling indicate a small or nil accretion rate (Lee et al. 1994). It is located in the same region as the two previous stars (see also map in Figure 13). Data are presented in Table 14 and Figure 14. The mean polarization at 7660 \AA , 0.2% at 72° , is mostly IS, as it is similar to the estimated IS polarization. Statistical tests do not indicate any variability.

6.11. Par 2494 = HBC 487 = NGC 1977 1069

Data for this 19.4815-day binary (Mathieu 1994) are presented in Table 15, Figures 15 and 16. This star is located in the same region as the three previous objects, where the IS reddening and polarization are low (see Table 3 and Figure 9). Since its position angle, 46° , does not correspond to the most common value for the less polarized stars measured by Breger (1976), nor to the IS position angle of 78° for stars with similar distances, part of the polarization is intrinsic, but IS polarization is also present.

The mean polarization at 7660 \AA , 0.16% at 46° , was determined to be statistically constant. Breger (1976) measured a polarization of $0.54 \pm 0.11\%$ at 69° , without any filter, which is above the mean of our measurements, but could be due to the wavelength dependence of the polarization. Data obtained with the polarimeter STERENN at the Pic-du-Midi Observatory (France) with a V filter and a 10° aperture hole on 29 January 1992 gives a polarization of $0.41 \pm 0.14\%$ at 52.5° (F. Ménard 2001, private communication), similar to Breger’s measurement and pointing to stability. Although all the available data point to a stable polarization, the binned data presented in Figure 16 show periodic variations, in position angle at least, and it is possible to get a reasonable fit when using equations 13 and 14. Since the statistical tests we used to check for the presence of variability do not take into account low amplitude but systematic variations such as those seen in the position angle for Par 2494, there could be periodic variations. The PDM and LNP find similar period of $\sim 38.5 \text{ d}$ for Par 2494, with a 70% chance that the data are not random Gaussian noise; this period is about twice the orbital period.

6.12. Ori 569 = ORINTT 569

This 4.25-day binary (Mathieu 1994) has a mass ratio of 1.00 ± 0.02 . The weak $H\alpha$ emission and absence of veiling indicate small or nil accretion rate (Lee et al. 1994). Lee (1992) discovered a third star in this system. Ori 569 is at about 3° from Ori 429 (see map in Figure 13). Data are presented in Table 18 and Figure 17. The mean polarization at 7660 \AA is 0.18% at 76° , very similar to the estimated IS polarization around this star ($0.21\% \pm 0.04$ at 90°). Statistical tests indicate possible variability, so we conclude that the observed polarization is a sum of intrinsic and IS polarizations.

6.13. W 134 = Walker 134 = NGC 2264 134 = VSB 92

Both components of this 6.3532-day binary are G stars showing strong $\text{Li I } 6707 \text{ \AA}$ absorption features; the total mass of the system is $M \sin^3 i = 3.16 M_\odot$ with a mass ratio of 1.04 (Padgett & Stapelfeldt 1994). It has a NIR excess more typical of CTTS, that can not be entirely attributed to dark spots, and that indicates some warm dust resides within 0.3 AU of the binary; on the

other hand, its weak emission lines make it a WTTS (Padgett & Stapelfeldt 1994). It has not been detected longward of $12\ \mu\text{m}$ so it probably does not have a CB disk (Jensen & Mathieu 1997).

When using an approximate $v \sin i$, the orbital period and the derived stellar radii, and the assumption that the system is tidally locked, the inclination is then $46^\circ \pm_{15}^{21}$ (Padgett & Stapelfeldt 1994). Theoretical masses give an orbital inclination of $63^\circ \pm 4$, which could be sufficient for grazing eclipses, given the stellar radii derived, but photometric monitorings during zero velocity separation events did not show any decrease in brightness (Padgett & Stapelfeldt 1994). Young (1978) reports $E(B - V) = 0.08$ mag for W 134 and notes that intra-cluster clouds not randomly distributed cause differential reddening, whereas Padgett & Stapelfeldt (1994) recalculated $E(B - V) = 0.2$ mag. Koch, Perry, & Kilambi (1994) report 0.35 mag variability in V and R , but no phase-locked variability could be found, and if present, could be hidden by non-periodic variations.

Polarization observations of 34 stars belonging to NGC 2264 (Corporon et al. in preparation) have an average position angle of 16° , whereas the average IS position angle of stars with similar distance to W 134 is 177° , different that W 134's value of 32° . A map of the polarization of neighboring stars is presented in Figure 18; the IS polarization vectors are mostly aligned to each other, indicating the presence of IS polarization (average of $0.87\% \pm 0.12\%$). Since W 134 shows polarimetric variations (see below), we conclude that its polarization is intrinsic with an IS component.

Data are presented in Table 16 and Figure 19, where the fit according to equations 13 and 14 is also shown. The average polarization, 0.22% at 32° , is statistically variable. In Figure 19, two atypical position angle values taken more than a year apart can be seen, near phase 0.55; such rapid changes are sometimes seen for eclipsing binaries (for example in the eclipsing binary EK Cep, Manset & Bastien in preparation). The grazing eclipses, predicted by Padgett & Stapelfeldt (1994) but not seen in photometry, should occur near phases 0.25 and 0.75. The rapid change in position angle is seen near phase 0.55 and not at the predicted phases for the eclipses; nonetheless, more polarimetric data should be taken near phase 0.55 to investigate the cause of the atypical polarimetric observations.

6.14. VSB 126 = NGC 2264 169

Data for this 12.924-day binary (Mathieu 1994) are presented in Table 17 and Figure 20. The mean polarization at $7660\ \text{\AA}$, 0.16% at 66° , is statistically constant. VSB 126 is within 0.2° of W 134 (see map in Figure 18), and therefore is also affected by an IS polarization component at 177° . Its low and constant polarization, with an average of 0.16% at 66° , is intrinsic with an IS component.

7. Orbital inclination

One of the goals of these polarimetric observations is to determine the orbital inclinations of the selected PMS binaries, by using the BME formalism. This formalism can still be used if the orbits are non-circular and the scatterers are spherical grains, within the limits presented in Papers I and II, and even if the BME formalism, with its first and second harmonics only, does not reproduce exactly the variations of eccentric systems.

Noise with a standard deviation greater than 10% of the amplitude of the polarimetric variations will prevent the BME formalism from finding a reasonable estimate of the true inclination (Paper I). Other studies have also shown that the quality of the data (number of data points, observational errors, amplitude of the polarimetric variations) can strongly influence the results found by the BME formalism.

Aspin, Simmons, & Brown (1981) have studied what standard deviation $\sigma_{\text{nec}}(i)$ is necessary to determine the inclination i to $\approx \pm 5^\circ$, with a 90% confidence level. They give an approximate relation for the data quality DQ :

$$DQ = \frac{\sigma_o}{A_o \sqrt{N_o}} = \frac{\sigma_{\text{nec}}(i)}{A(i) \sqrt{N}}, \quad (17)$$

where

$$A = \frac{|Q_{\text{max}} - Q_{\text{min}}| + |U_{\text{max}} - U_{\text{min}}|}{4}, \quad (18)$$

σ_o is the observational error on the polarization, A_o is the observed polarimetric variability calculated with Equation 18, N_o is the number of observations, and $N = 40$ (the number of bins in their simulations). A set of very good quality observations will have a low value of DQ . We present in Table 19, Column 2, DQ values for the binaries studied here. After the quantity $\sigma_{\text{nec}}(i)/A(i)$ is calculated, Table 1 in Aspin et al. (1981) gives the lowest possible inclination that can be determined from the observations with a $\pm 5^\circ$ accuracy at a significance of 10% (meaning that the true inclination has a probability of 90% to be in within 5° of the value returned by the BME formalism). If we apply this method to our sets of data, we find that the quality of our data do not allow us to find i to $\approx \pm 5^\circ$, with a 90% confidence level, for any of our binaries.

Wolinski & Dolan (1994) have also studied the confidence intervals for orbital parameters determined polarimetrically. They made Monte Carlo simulations of noisy polarimetric observations, for a specific geometry not suitable for the stars studied in this present paper, but their results are nonetheless instructive. Confidence intervals for i are given graphically as a function of a “figure of merit” γ :

$$\gamma = \left(\frac{A}{\sigma_p} \right)^2 \left(\frac{N}{2} \right), \quad (19)$$

where σ_p is the standard deviation of the noise that was added to the data and N is the number of observations. We have calculated and present in Column 3 of Table 19 the figures of merit γ for some PMS binaries, by using the observational error $\sigma(P)$ instead of the σ_p used by Wolinski &

Dolan. It is again seen that the quality of the data is not very good, mostly because the amplitude A is rather low (between 0.02 and 0.10% in general).

Finally, following our own studies of the effects of noise on the BME results (Paper I), we have calculated the noise for the Stokes parameters Q and U , by using the variance of the fit and the amplitude of the polarimetric variations; these amplitudes are computed from the maximum and minimum values of the observations, and not those of the fit. These calculations are presented in Columns 4 and 5 of Table 19, where levels of noise below 10% are rare. Once again, this analysis shows that the polarimetric observations of PMS stars are not of “very good quality”, not because of instrumental or observational problems, but because non-periodic stochastic polarization variations and low amplitude periodic variations make the data rather noisy, hiding the periodic polarimetric variations that most probably exist.

One of the stars for which the polarimetric variations are very clear and might be of good enough quality for the BME formalism to work is AK Sco (Manset & Bastien, in preparation); this star is the only one for which the data were obtained within a few (12) consecutive nights. All the other stars were observed over 3-5 years. For these, non periodic polarimetric events, or changes in the circumstellar environment from epoch to epoch, mask the periodic variations and introduce too much noise. Future observations should be obtained at a site offering many consecutive clear nights to cover in one run the whole orbital period.

Assuming the BME formalism can be used to analyze the polarimetric variations of binary PMS stars, we have added in Table 19 the results of the BME analysis for the orbital inclination. Most of the inclinations are near 90° , which cannot be a real result. This is compatible with the above discussion on the effects of the stochastic noise on the inclination analysis, and does not necessarily mean that the BME analysis can not be used for these systems.

8. Orientation of the orbital plane and moments of the distribution of the scatterers

In addition to the orbital inclination, the BME formalism returns Ω , the orientation of the orbital plane with respect to the plane of the sky, and moments of the distribution of the scatterers, which are used to measure the asymmetry with respect to the orbital plane ($\tau_0 G$), and the degree of concentration towards the orbital plane ($\tau_0 H$). It is generally expected that the distribution will be symmetric and concentrated in the orbital plane, so $\tau_0 H > \tau_0 G$. In Table 20, we present the values of Ω , $\tau_0 H$, $\tau_0 G$, and the ratio $\tau_0 H / \tau_0 G$. If the circumbinary disks of these binaries can be imaged (with interferometric or adaptive optics techniques), their orientation should be similar to Ω , although the orbits are not necessarily coplanar with the disks or envelopes. The values for $\tau_0 G$ and $\tau_0 H$ are similar to those we have found in numerical simulations (Paper I), and to the observed values for other types of binaries (Bastien 1988; Koch et al. 1994). In particular, $\tau_0 H > \tau_0 G$ as expected, with ratios approximately from 1.0 to 4.0.

These parameters are also calculated using the coefficients of the fits and the same assumptions

(the scatterers are electrons, the orbits are circular). However, single-periodic variations that are not present when the scatterers are electrons and the orbits are circular, do appear in our simulations when there are dust grains instead of electrons, variable optical depth effects are considered, or the orbits are eccentric (Paper I and II). Therefore, the values of the parameters calculated might not reflect an asymmetric configuration ($\tau_0 G$) or a concentration toward the orbital plane ($\tau_0 H$). For example, we have found, using the code presented in Papers I and II, that even though $\tau_0 G$ should be null for a perfectly symmetric configuration, it will not be if we have dust grains or consider variable optical depth effects.

9. Discussion

We have presented polarimetric observations for 14 spectroscopic PMS binaries located in the Taurus, Auriga, and Orion SFRs. The majority of the PMS binaries observed have a detectable linear polarization; only LkCa 3, NTTS 045251+3016, Ori 569, and VSB 126 do not present polarization levels above the 3σ limit. For most binaries, IS polarization is also an important component of the observations. After an estimation of this IS polarization is removed, a few (5 out of 14) of the binaries present clear indications of intrinsic polarizations $\gtrsim 0.5\%$ and significantly above the IS polarization: V826 Tau, UZ Tau E/W, DQ Tau, GW Ori, and Par 1540. Overall, 7 of our 14 binaries, including all the clearly identified CTTS binaries (UZ Tau E, DQ Tau, and GW Ori; Mathieu et al. 1997), show intrinsic polarizations above 0.5%. Interestingly, then, even the WTTS and NTTS, for which other types of observations are not indicative of significant amounts of circumstellar material, can have detectable levels of polarization.

As has been found for single PMS stars, the polarization of PMS binaries is variable. All binaries are statistically variable or suspected variable, except LkCa 3, NTTS 045251+3016, Par 2494, Ori 429, and VSB 126. Despite the results of those tests, graphs of polarimetric data as a function of orbital phase show that LkCa 3 could be variable in position angle, and Par 2494 is clearly variable in θ . Not enough data are available for DQ Tau to determine its variability. When combining data from literature and our two observations for UZ Tau E/W, variability is present. Therefore, we find that 54% of the PMS binaries are variable (7 of out 13), or 77% (10 out of 13) variable or possibly so; these results are compatible with those of Bastien (1988) and Ménard & Bastien (1992). All the known CTTS binaries in our sample (except maybe DQ Tau for which we only have one measurement) present polarimetric variations. Many NTTS or WTTS also show polarimetric variations. Therefore, around these stars, although it is not thought that there is much CS material, there is enough to produce polarimetric variations, as it can be shown that very little mass in the form of dust is needed to produce detectable levels of polarization.

Some stars have shown, once or even a few times, atypical values of polarization and/or position angle that are well below or above the rest of the data (Par 1540, Par 2494, and also MWC 1080, Paper III). We believe these are real observations of events that strongly affected the stars and/or their environment. Single PMS stars are known sometimes to be strongly variable, so this is not a

surprise. For the stars with a sufficient amount of data, additional observations at similar phases indicate that these atypical points are not related to the normal periodic behavior. Photometry or spectroscopy obtained at the same times as those of the atypical observations could help reveal the cause.

Only 6 binaries have enough observations to investigate the presence of periodic polarimetric variations: LkCa 3, V826 Tau, GW Ori, Par 1540, Par 2494, and W 134. Statistical tests conclude that LkCa 3's and Par 2494's polarization is constant, but low amplitude periodic variations are nonetheless present. The position angle for LkCa 3's polarization outlines a sinusoidal wave between phases 0.2 and 0.65; since the data were obtained over 22 months, representing more than 600 orbits, it cannot be attributed to coincidence, but to a real variation. Although Par 2494's observations are rather noisy, binned data reveal low amplitude periodic variations in position angle. Therefore, low amplitude variations, especially if masked by noise, can be missed by statistical tests for variability, because these only consider the whole of the observations without their known order (as a function of phase).

A third binary, Par 1540, shows periodic variations, although they also are of low amplitude. Period analysis for Par 1540 and Par 2494, with PDM and LNP, confirm that the periodicity is due to the orbital motion, although not with a very high significance. Non-periodic or pseudo-periodic polarimetric variations could explain why it is difficult to see periodic variations and confirm them with period analysis methods. Those non-periodic variations may be caused by appearance or disappearance of hot or cool spots, flares, or major changes in the distribution or density of matter in the CS or CB environment. To avoid or at least decrease the effects of those events, observations should be carried on consecutive nights before any major stochastic change in polarization occurs, and until the orbital period has been sufficiently covered. Those three PMS binaries which exhibit low amplitude polarimetric variations are WTTS; this indicates that there is still enough dust in their environment to produce polarization and periodic variations.

A fourth interesting case is W 134, which may be an eclipsing system: two atypical position angles, taken more than a year apart, are seen near phase 0.55; such rapid changes are sometimes seen for eclipsing binaries (for example in the eclipsing binary EK Cep, Manset & Bastien in preparation; see also St-Louis et al. 1993). The rapid change in position angle is not at the predicted phases for the eclipses; nonetheless, more polarimetric data should be taken near phase 0.55 to investigate the cause of the atypical polarimetric observations.

One of the goals of these observations was to find the orbital inclinations. Unfortunately, non-periodic or pseudo-periodic variations sometimes mask the truly periodic variations by introducing noise. This noise, as measured by 3 different methods, is too high for the BME formalism to find reasonable estimates of the orbital inclination. Three factors contribute to this difficulty. First, dust grains are the main scatterers in these systems, and it has been shown that dust grain produce polarimetric variations of smaller amplitude than electrons (Paper II). Second, the disk around these short-period binaries are probably CB rather than CS ones, and CB disks produce variations

of smaller amplitudes than CS disks (Paper II). Finally, non-periodic events introduce noise that masks the already small amplitude variations. This last problem might only be improved by taking data on shorter periods of time.

Other parameters are returned by the BME formalism: Ω , the orientation of the orbital plane with respect to the plane of the sky, and moments of the distribution of the scatterers, used to measure the asymmetry with respect to the orbital plane ($\tau_0 G$), and the degree of concentration towards the orbital plane ($\tau_0 H$). Although the assumptions used in the BME formalism (scattering on electrons, circular orbits) are not met in the PMS binaries studied here and we have shown that even in simple cases the values are incorrect, the values returned for PMS binaries are of the same order of magnitude as values for other types of stars and as for our simulations.

A similar detailed analysis will be presented for PMS binaries in the Scorpion and Ophiucus SFRs in a coming paper.

N. M. thanks the directors of the Mont Mégantic Observatory for granting generous time over many years. The technical support from the technicians of the observatory, B. Malenfant, G. Turcotte, and F. Urbain is duly acknowledged. We thank F. Ménard for providing unpublished data for Par 1540 and Par 2494. N. M. thanks the Conseil de Recherche en Sciences Naturelles et Génie of Canada, the Fonds pour la Formation de Chercheurs et l'Aide à la Recherche of the province of Québec, the Faculté des Etudes Supérieures and the Département de physique of Université de Montréal for scholarships, and P. B. for financial support. We thank the Conseil de Recherche en Sciences Naturelles et Génie of Canada for supporting this research. N. M. is Guest User, Canadian Astronomy Data Centre, which is operated by the National Research Council, Herzberg Institute of Astrophysics, Dominion Astrophysical Observatory.

REFERENCES

- Aspin, C., Simmons, J. F. L., & Brown, J. C. 1981, MNRAS, 194, 283
- Basri, G., & Batalha, C. 1990, ApJ, 363, 654
- Bastien, P. 1982, A&AS, 48, 153
- Bastien, P. 1985, ApJS, 59, 277
- Bastien, P. 1988, in Polarized Radiation of Circumstellar Origin, ed. G. V. Coyne et al. (Tucson, AZ: University of Arizona Press), 595
- Bastien, P. 1996, in ASP Conf. Ser. 97, Polarimetry in the Interstellar Medium, ed. W. G. Roberge & D. C. B. Whittet (San Francisco: ASP), 297
- Bastien, P., Drissen, L., Ménard, F., Moffat, A. F. J., Robert, C., & St-Louis, N. 1988, AJ, 95, 900
- Bertout, C. 1989, ARA&A, 27, 351
- Bouvier, J., & Bertout, C. 1989, A&A, 211, 99
- Bouvier, J., Cabrit, S., Fernández, M., Martín, E. L., & Matthews, J. M. 1993, A&A, 272, 176
- Breger, M. 1974, ApJ, 188, 53
- Breger, M. 1976, ApJ, 204, 789
- Breger, M., Gehrz, R. D., & Hackwell, J. A. 1981, ApJ, 248, 963
- Brooks, A., Clarke, D., & McGale, P. A. 1994, Vistas in Astronomy, 38, 377
- Brown, J. C., Mclean, I. S., & Emslie, A. G. 1978, A&A, 68, 415
- Catala, C. 1989, in ESO Conf. Proc. 33, Low Mass Star Formation and Pre-Main-Sequence Evolution, ed. B. Reipurth (Garching bei München: ESO), 471
- Clarke, D., & Naghizadeh-Khouei, J. 1994, AJ, 108, 687
- Drissen, L., Bastien, P., & St-Louis, N. 1989, AJ, 97, 814
- Dutrey, A., Guilloteau, S., Duvert, G., Prato, L., Simon, M., Schuster, K., & Ménard, F. 1996, A&A, 309, 493
- Feigelson, E. D., Welty, A. D., Imhoff, C. L., Hall, J. C., Etzel, P. B., Phillips, R. B., & Lonsdale, C. J. 1994, ApJ, 432, 373
- Ghez, A., Neugebauer, G., & Matthews, K. 1993, AJ, 106, 2005
- Grankin, K. N. 1993, IAU Information Bulletin on Variable Stars, no 3823

- Grinin, V., Kolotilov, E. A., & Rostopchina, A. 1995, *A&AS*, 112, 457
- Grinin, V. P., Kisilev, N. N., Minikhulov, N. H., Chernova, G. P., & Voshchinnikov, N. V. 1991, *Ap&SS*, 186, 283
- Heiles, C. 2000, *AJ*, 119, 923
- Herbig, G. H., & Bell, K. R. 1988, *Lick Obs. Bull.* 1111, 1
- Herbst, W. 1989, *AJ*, 98, 2268
- Hough, J. H., Bailey, J., Cunningham, E. C., McCall, A., & Axon, D. J. 1981, *MNRAS*, 195, 429
- Jensen, E. L. N., & Mathieu, R. D. 1997, *AJ*, 114, 301
- Jensen, E. L., Mathieu, R. D., & Fuller, G. A. 1994, *ApJ*, 429, 29
- Jensen, E. L., Mathieu, R. D., & Fuller, G. A. 1996a, *ApJ*, 458, 312
- Jensen, E. L., Koerner, D. W., & Mathieu, R. D. 1996b, *AJ*, 111, 2431
- Jones, B. F., & Walker, M. F. 1988, *AJ*, 95, 1755
- Koch, R. H., Perry, P. M., & Kilambi, G. C. 1994, *IAU Information Bulletin on Variable stars*, no 4032
- Lee, C. W. 1992, Ph.D. thesis, University of Wisconsin
- Lee, C. W., Martín, E. L., & Mathieu, R. D. 1994, *AJ*, 108, 1445
- Leinert, Ch., Zinnecker, H., Weitzel, N., Christou, J., Ridgway, S. T., Jameson, R., Haas, M., & Lenzen, R. 1993, *A&A*, 278, 129
- Manset, N. 2000, Ph.D. thesis, Université de Montréal
- Manset, N., & Bastien, P. 1995, *PASP*, 107, 483
- Manset, N., & Bastien, P. 2000, *AJ*, 120, 413 (Paper I)
- Manset, N., & Bastien, P. 2001a, *AJ*, 122, 2692 (Paper II)
- Manset, N., & Bastien, P. 2001b, *AJ*, 122, 3453 (Paper III)
- Marshall, L. A., & Mathieu, R. D. 1988, *AJ*, 96, 1956
- Mathewson, D. S., Ford, V. I., Klare, G., Neckel, TH., & Krautter, J. 1978, *BICDS*, 14, 115
- Mathieu, R. D. 1994, *ARA&A*, 32, 465
- Mathieu, R. D., Walter, F. M., & Myers, P. C. 1989, *AJ*, 98, 987

- Mathieu, R. D., Adams, F. C., & Latham, D. W. 1991, *AJ*, 101, 2184
- Mathieu, R. D., Martin, E. L., & Maguzzu, A. 1996, *BAAS*, 188, 6005
- Mathieu, R. D., Adams, F. C., Fuller, G. A., & Jensen, E. L. 1993, *BAAS*, 182, 62.20
- Mathieu, R. D., Adams, F. C., Fuller, G. A., Jensen, E. L. N., Koerner, D. W., & Sargent, A. I. 1995, *AJ*, 109, 2655
- Mathieu, R. D., Stassun, K., Basri, G., Jensen, E. L., Johns-Krull, C. M., Valenti, J. A., & Hartmann, L. W. 1997, *AJ*, 113, 1841
- Ménard, F., & Bastien, P. 1992, *AJ*, 103, 564
- Mundt, R., Walter, F. M., Feigelson, E. D., Finkenzeller, U., Herbig, G. H., & Odell, A. P. 1983, *ApJ*, 269, 229
- Padgett, D. L., & Stapelfeldt, K. R. 1994, *AJ*, 107, 720
- Press, W. H., Teukolsky, S. A., Vetterling, W. T., & Flannery, B. P. 1997, *Numerical Recipes in C, The Art of Scientific Computing*, 2d edition (Cambridge: Cambridge University Press)
- Reipurth, B., Lindgren, H., Nordstrom, B., & Mayor, M. 1990, *A&A*, 235, 197
- Robert, C., Moffat, A. F. J., Bastien, P., St-Louis, N., & Drissen, L. 1990, *ApJ*, 359, 211
- Robert, C., et al. 1992, *ApJ*, 397, 277
- Rudy, R. J., & Kemp, J. C. 1978, *ApJ*, 221, 200
- Rydgren, A. E., & Vrba, F. J. 1983a, *AJ*88, 1017
- Rydgren A. E., & Vrba, F. J. 1983b, *ApJ*, 267, 191
- Serkowski, K. 1958, *Acta Astronomica*, 8, 135
- Shevchenko, V. S., Grankin, K. N., Ibragimov, M. A., & Melnikov, S. Yu. 1992, *IAU Information Bulletin on Variable stars*, no 3746
- Schneeberger, T. J., Worden, S. P., & Wilkerson, M. S. 1979, *ApJS*, 41, 369
- Simon, M., & Prato, L. 1995, *ApJ*, 450, 824
- Skinner, S. L., Brown, A., & Walter, F. M. 1991, *AJ*, 102, 1742
- Stassun, K., Mathieu, R. D., Basri, G., Johns-Krull, C. M., Valenti, J. A., Jensen, E. L., & Hartmann, L. W. 1996, *BAAS*, 188, 4006
- Stellingwerf, R. F. 1978, *ApJ*, 224, 953

- St-Louis, N., Moffat, A. F. G., Lapointe, L., Efimov, Yu. S., Shakhovskoy, N. M., Fox, G. K., & Piirola, V. 1993, *ApJ*, 410, 342
- Topping, J. 1972, *Errors of Observation and their Treatment* (London: Chapman and Hall)
- Weaver, W. B., & Jones, G. 1992, *ApJS*, 78, 239
- Walter, F. M. 1986, *ApJ*, 306, 573
- Walter, F. M., Brown, A., Mathieu, R. D., Myers, P. C., & Vrba, F. J. 1988, *AJ*, 96, 297
- Welty, A. D. 1995, *AJ*, 110, 776
- Wolinski, K. G., & Dolan, J. F. 1994, *MNRAS*, 267, 5
- Wolk, S. J., & Walter, F. M. 1996, *AJ*, 111, 2066
- Young, A. 1978, *PASP*, 90, 144
- Yudin, R. V. 2000, *A&A Suppl. Series*, 144, 285
- Zakirov, M. M., Azimov, A. A., & Grankin, K. N. 1993, *IAU Information Bulletin on Variable stars*, no 3898

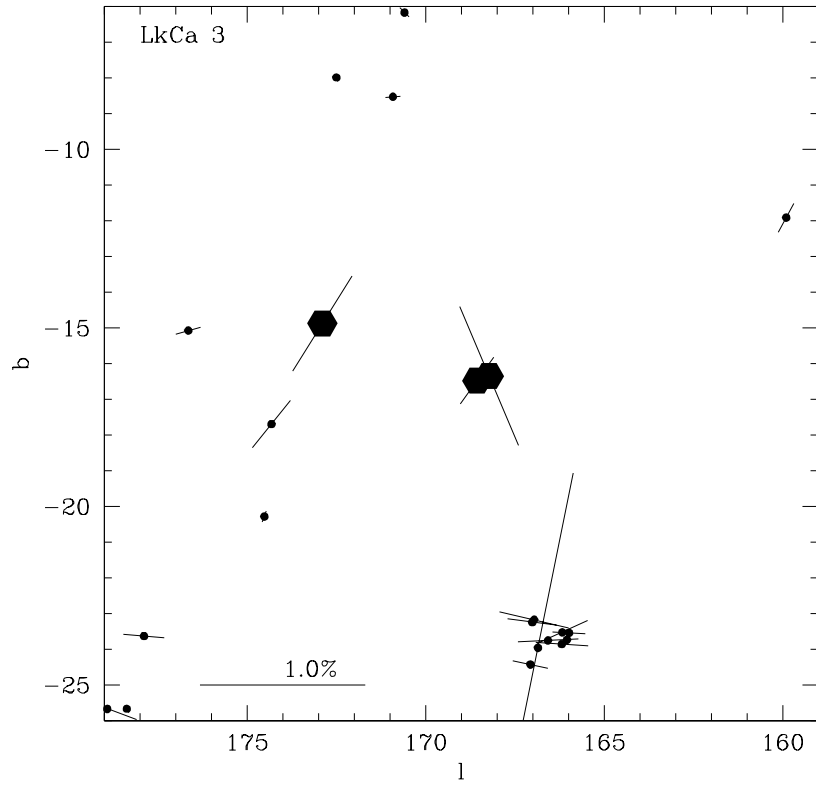


Fig. 1.— Map of the interstellar polarization in the vicinity of V773 Tau (hexagonal symbol at right), LkCa 3 (at the center of the map), and UZ Tau (left). The stars selected to calculate the IS polarization are within 70 pc of those targets.

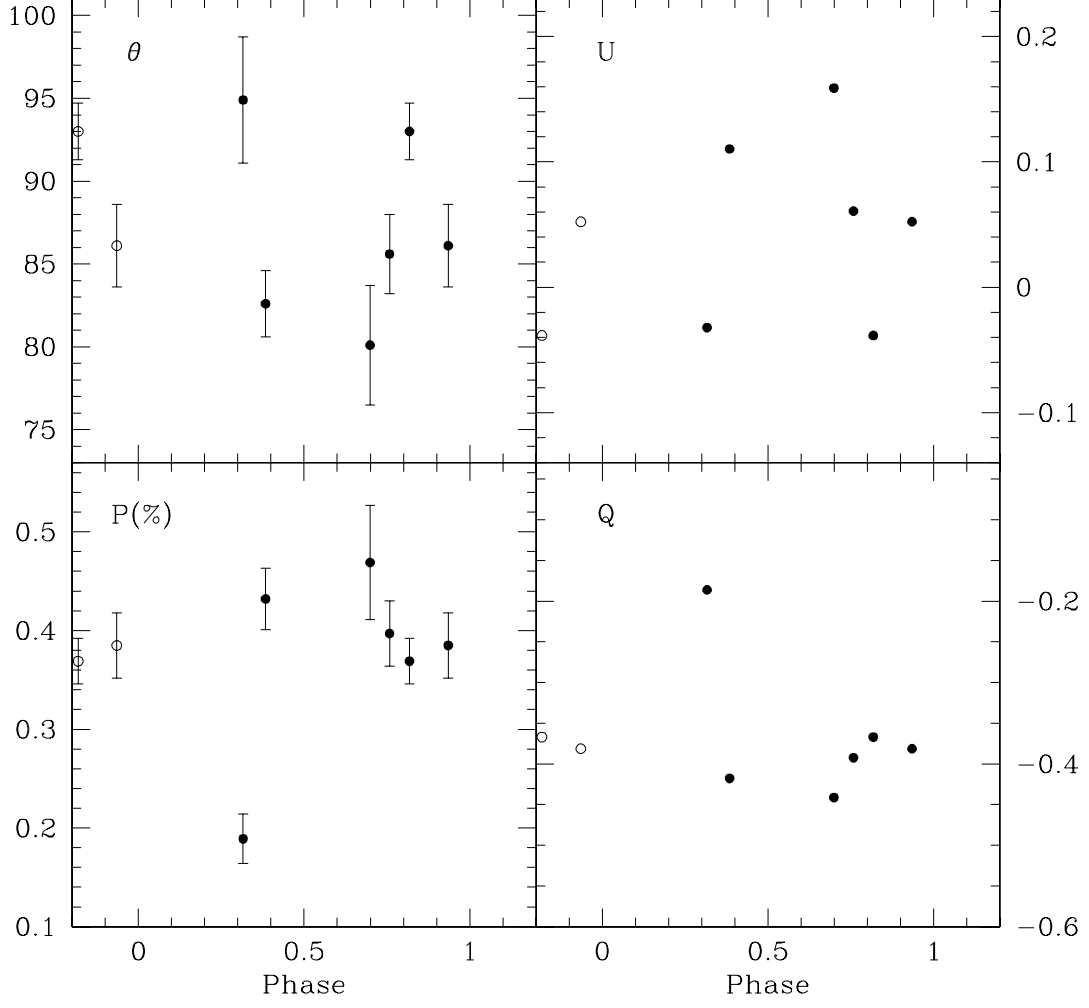


Fig. 2.— Polarimetric observations of V773 Tau. This star is polarimetrically variable.

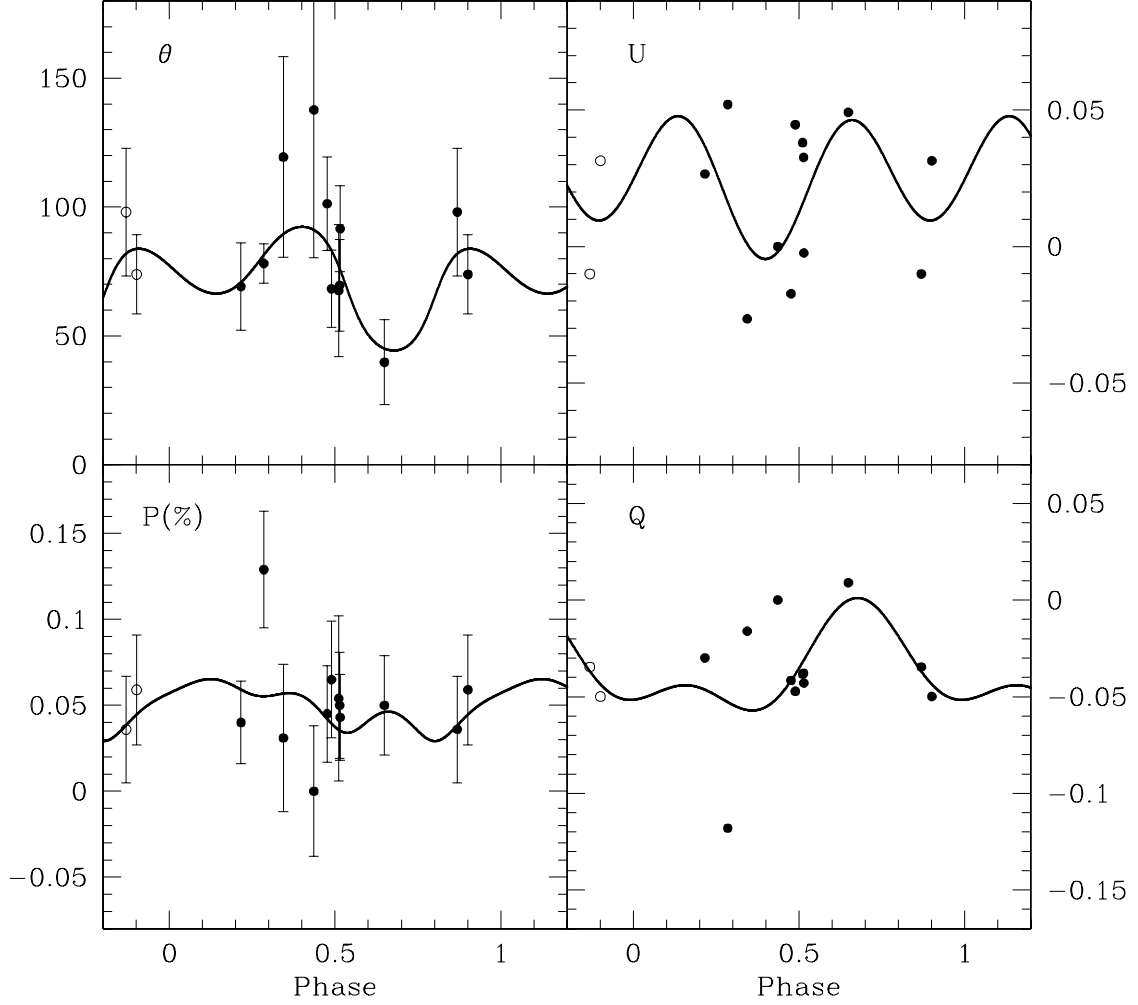


Fig. 3.— Polarimetric observations of LkCa 3. Statistical tests determined its polarization is constant, although there seems to be a sinusoidal trend in polarization angle between phases 0.2 and 0.65.

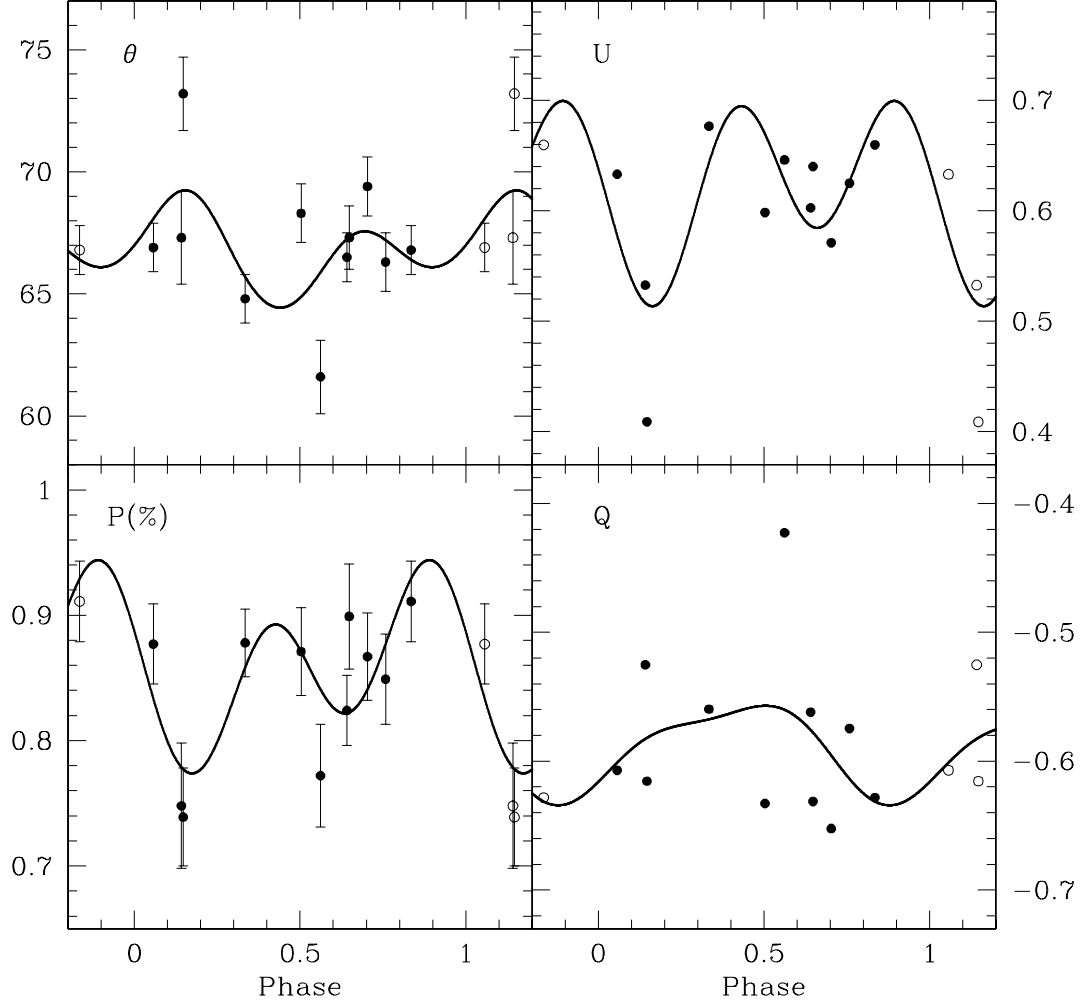


Fig. 4.— Polarimetric observations of V826 Tau, a polarimetrically variable binary.

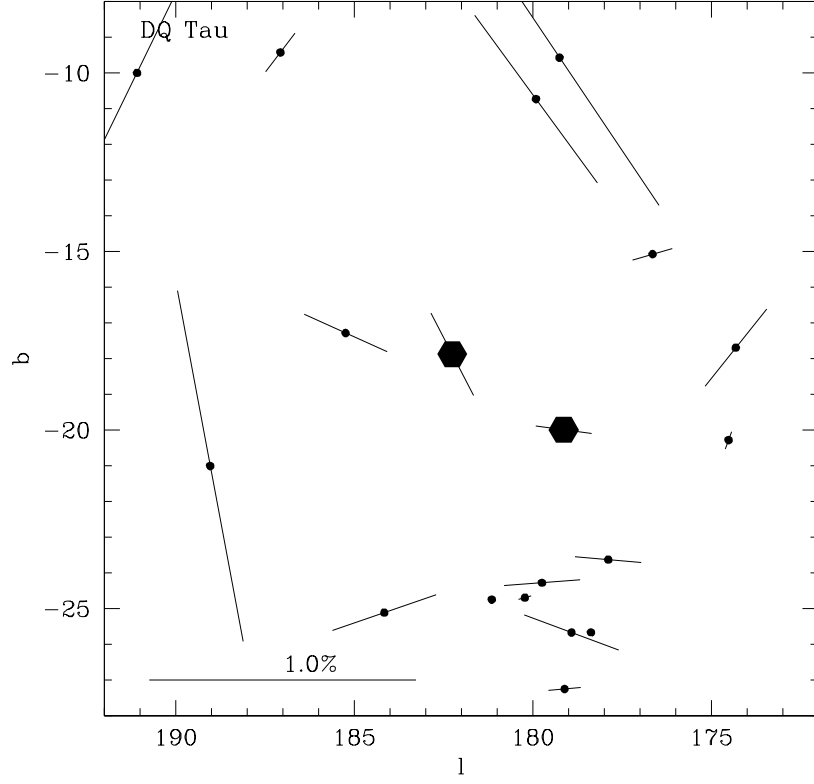


Fig. 5.— Map of the interstellar polarization in the vicinity of V826 Tau (hexagonal symbol at right) and DQ Tau (at the center of the map). The stars selected to calculate the IS polarization are within 80 pc of those targets.

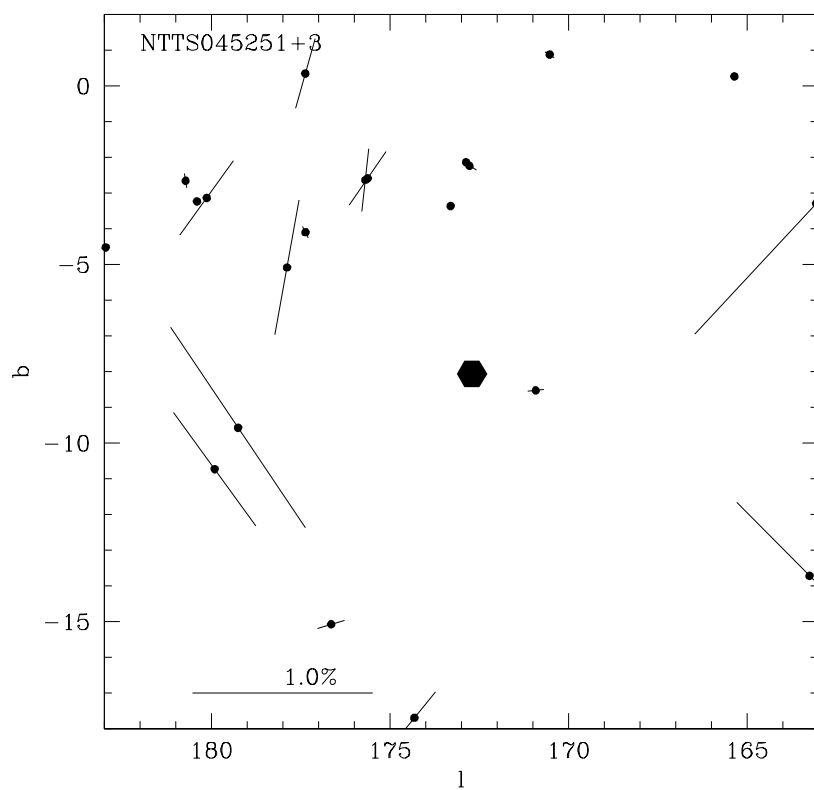


Fig. 6.— Map of the interstellar polarization in the vicinity of NTTS 045251+3016. The stars selected to calculate the IS polarization are within 80 pc of this target.

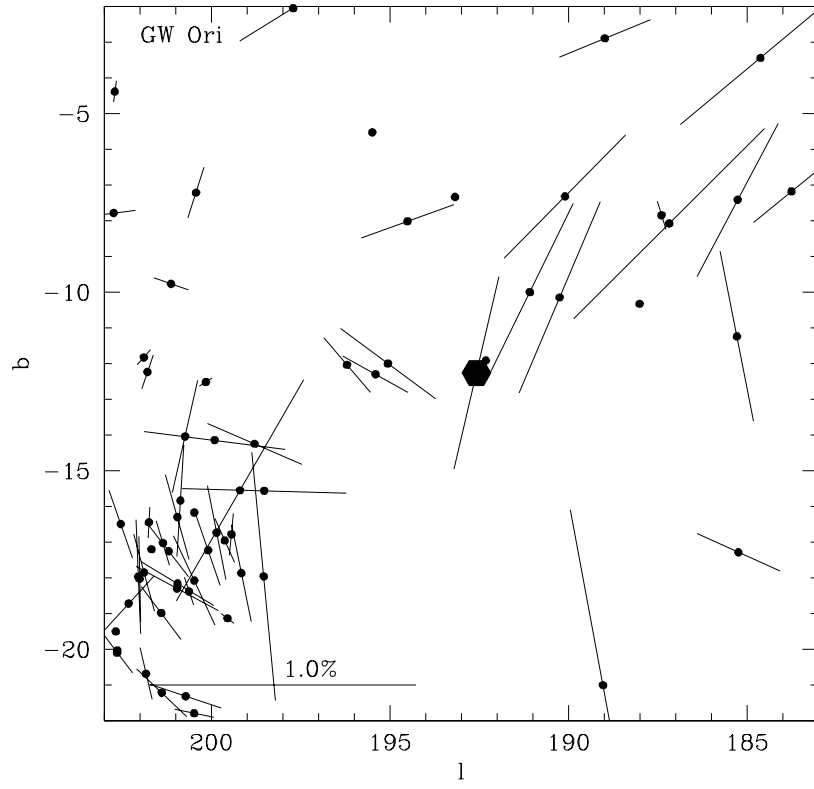


Fig. 7.— Map of the interstellar polarization in the vicinity of GW Ori. The stars selected to calculate the IS polarization are within 200 pc of this target.

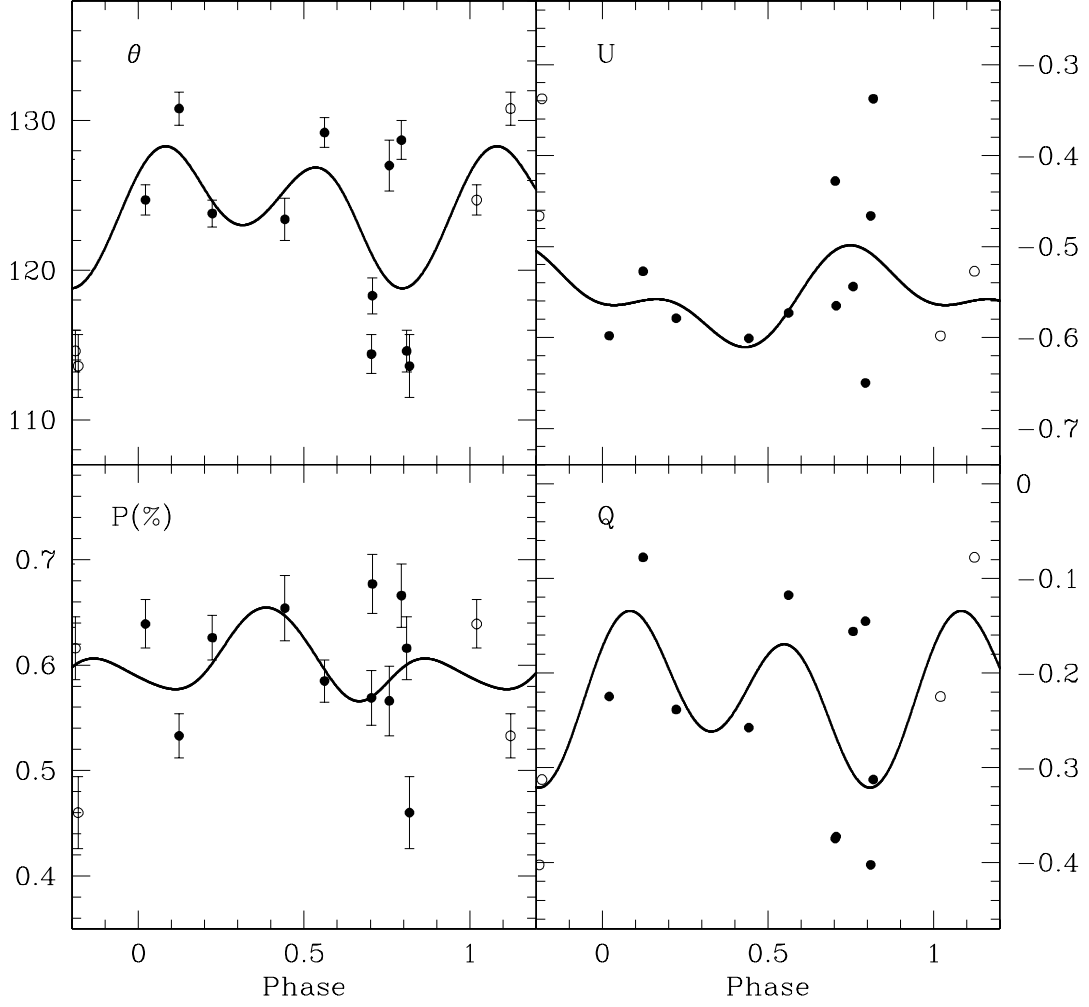


Fig. 8.— Polarimetric observations of GW Ori. This star is polarimetrically variable.

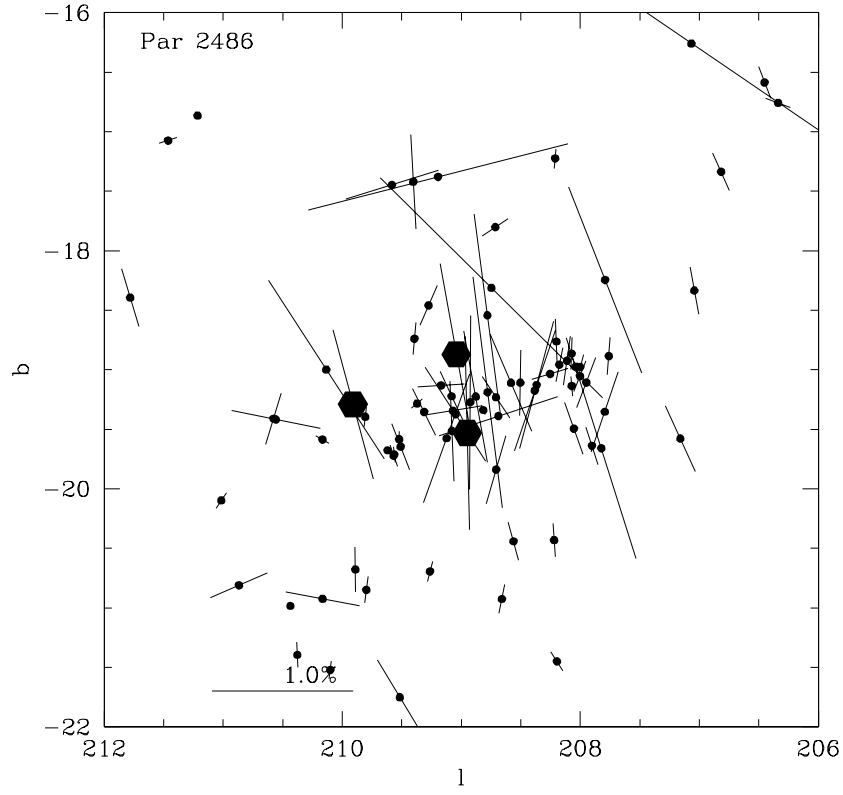


Fig. 9.— Map of the interstellar polarization in the vicinity of Par 2486 (at the center of the map), Par 1540 (below center), and Par 2494 (left). The stars selected to calculate the IS polarization are within 235 pc of those targets.

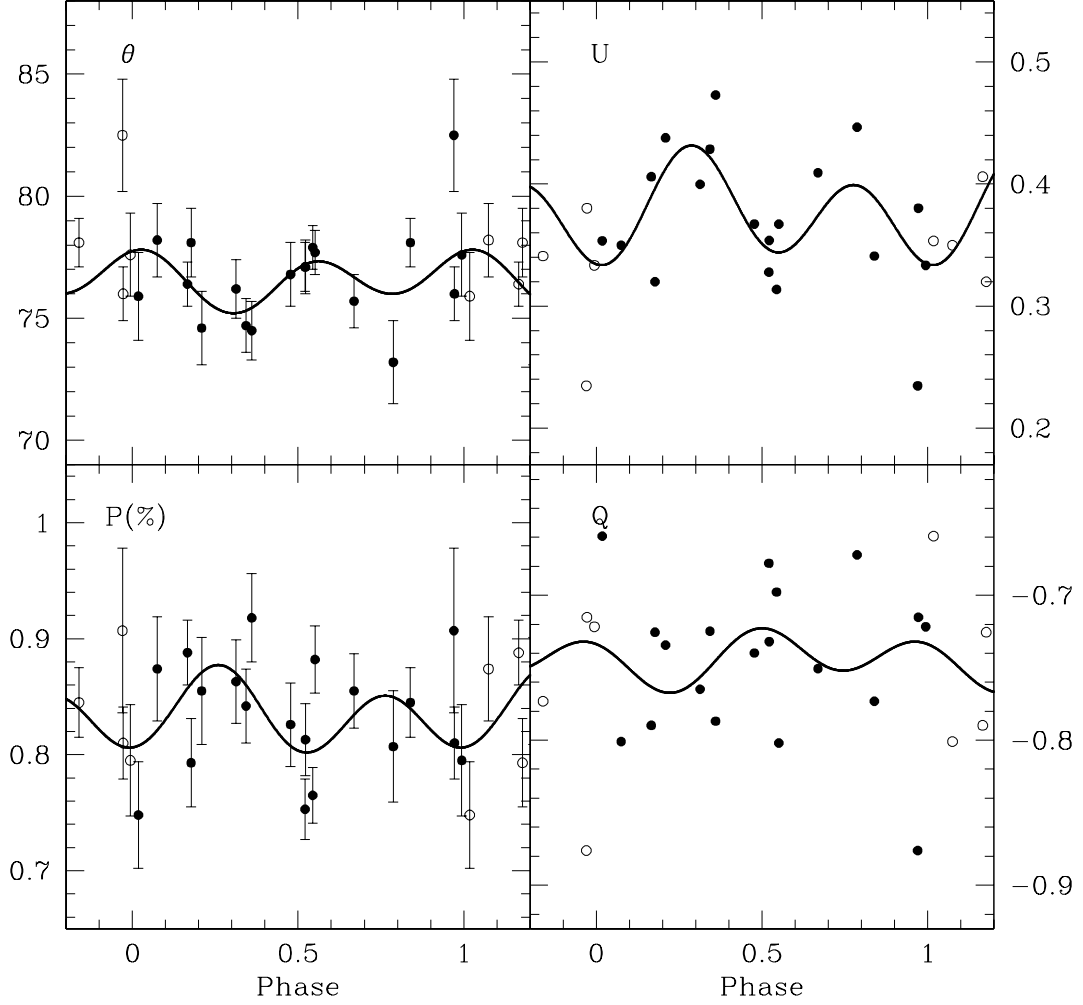


Fig. 10.— Polarimetric observations of Par 1540; one point with a rather high polarization of $\approx 1.1\%$ was removed. Clearly, this binary is variable, but there is a lot of scatter, and periodic variations are not clear.

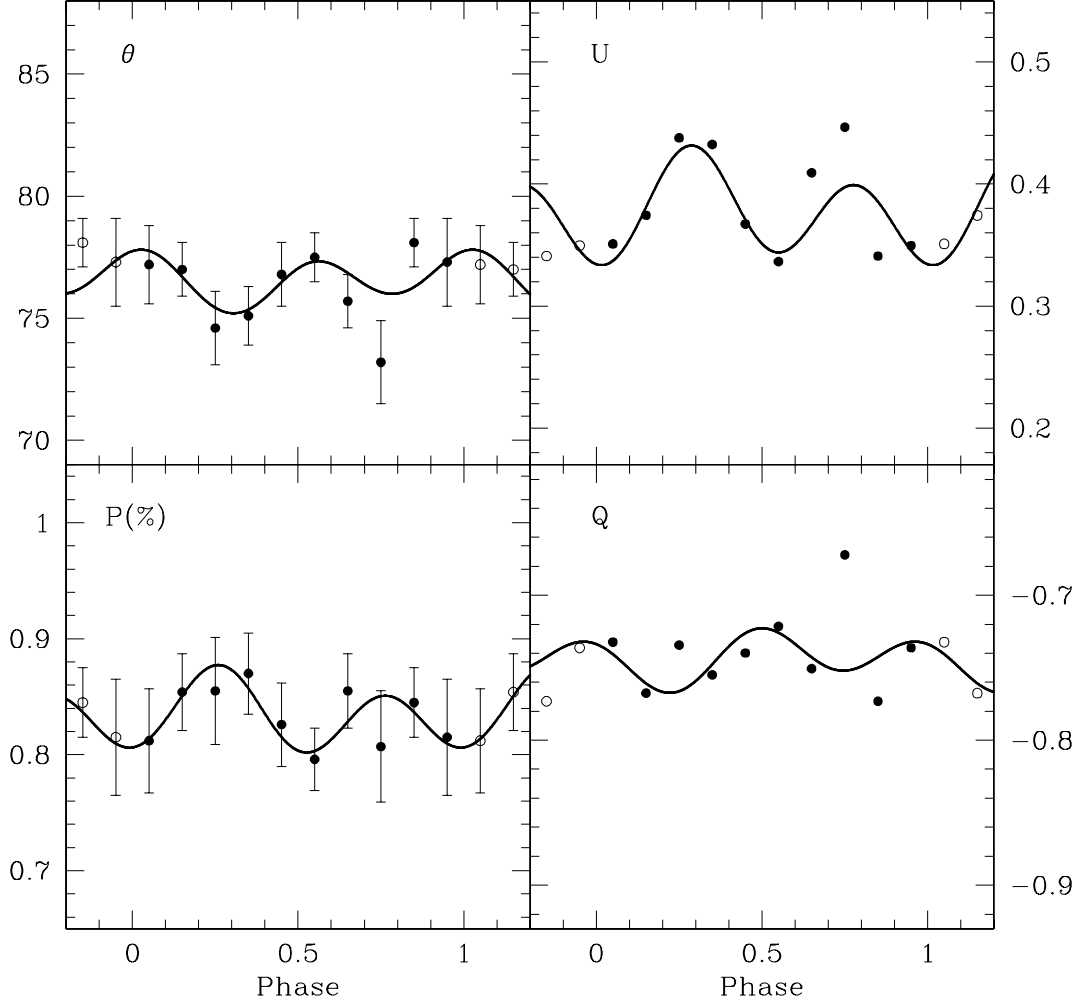


Fig. 11.— Polarimetric observations of Par 1540. Data have been binned in phase, to reveal small amplitude periodic variations.

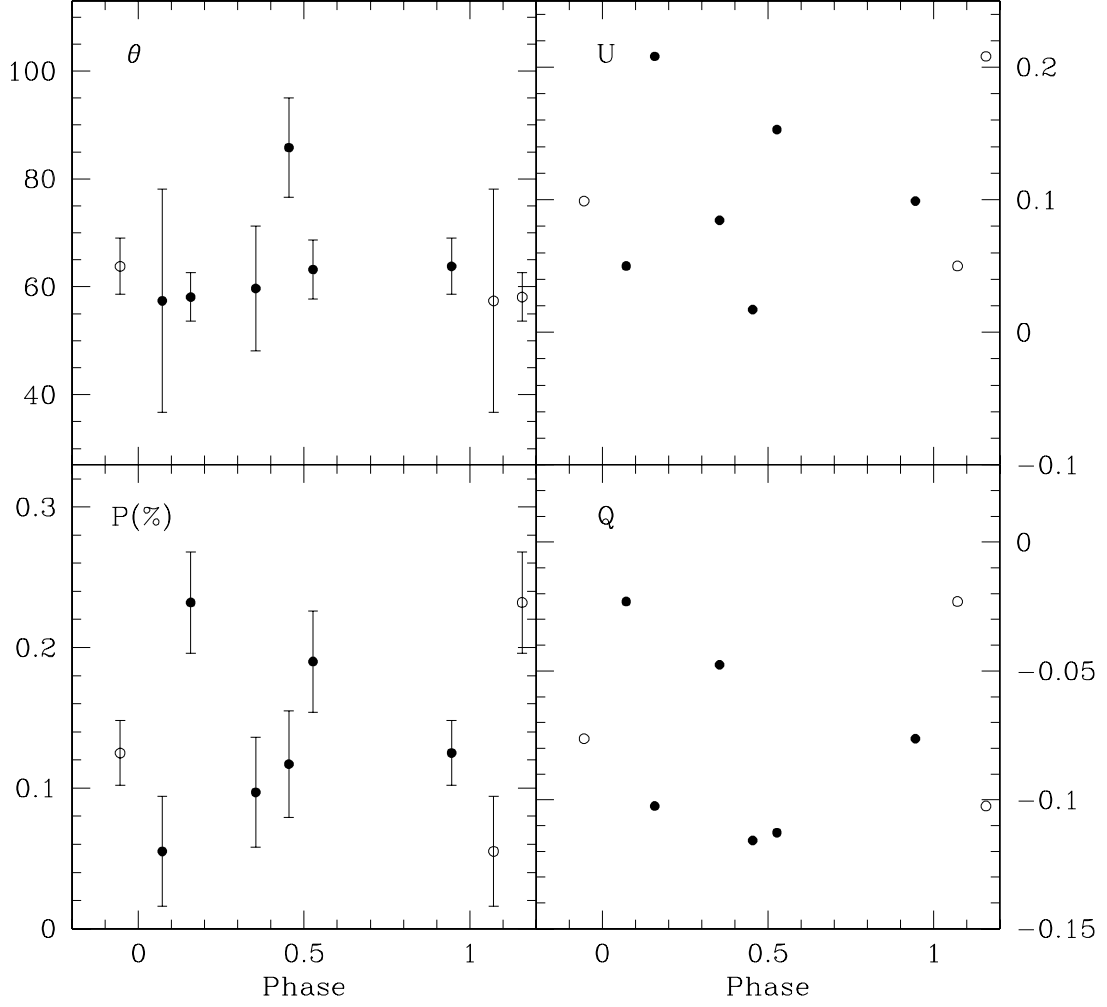


Fig. 12.— Polarimetric observations of Par 2486.

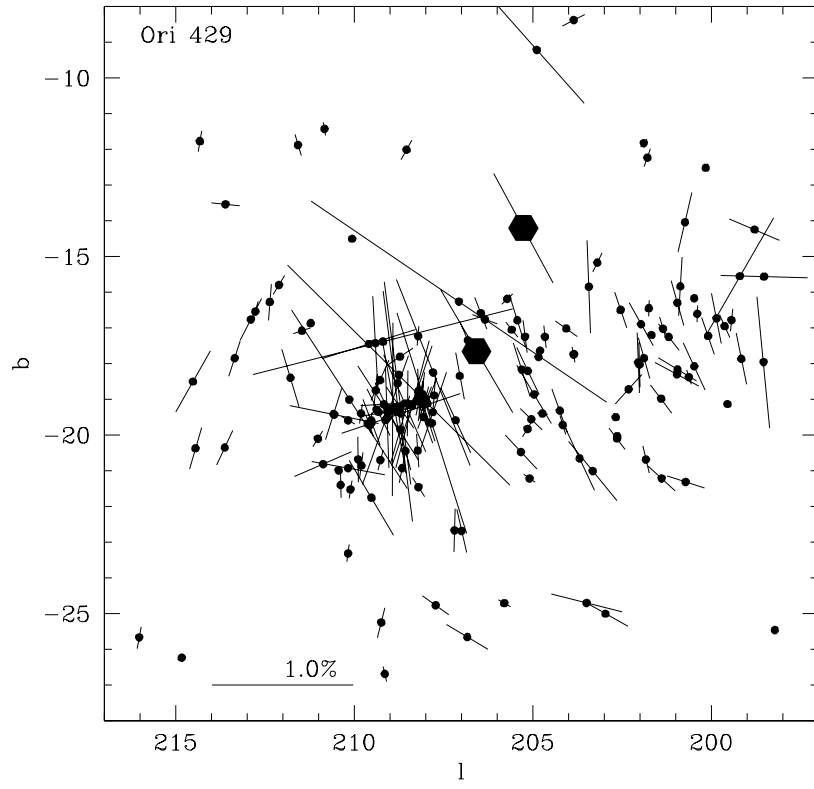


Fig. 13.— Map of the interstellar polarization in the vicinity of Ori 429 (at the center of the map) and Ori 569 (above center). The stars selected to calculate the IS polarization are within 235 pc of those targets.

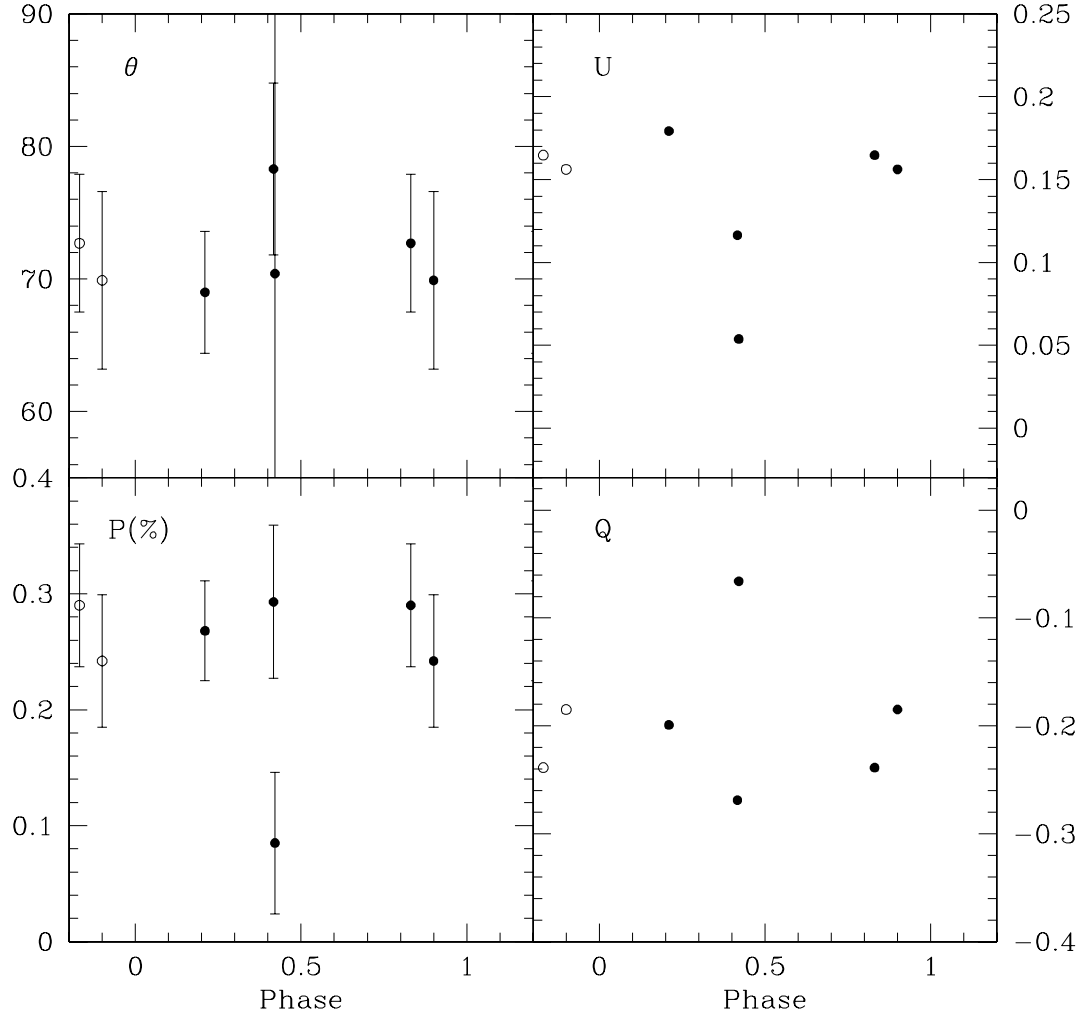


Fig. 14.— Polarimetric observations of Ori 429.

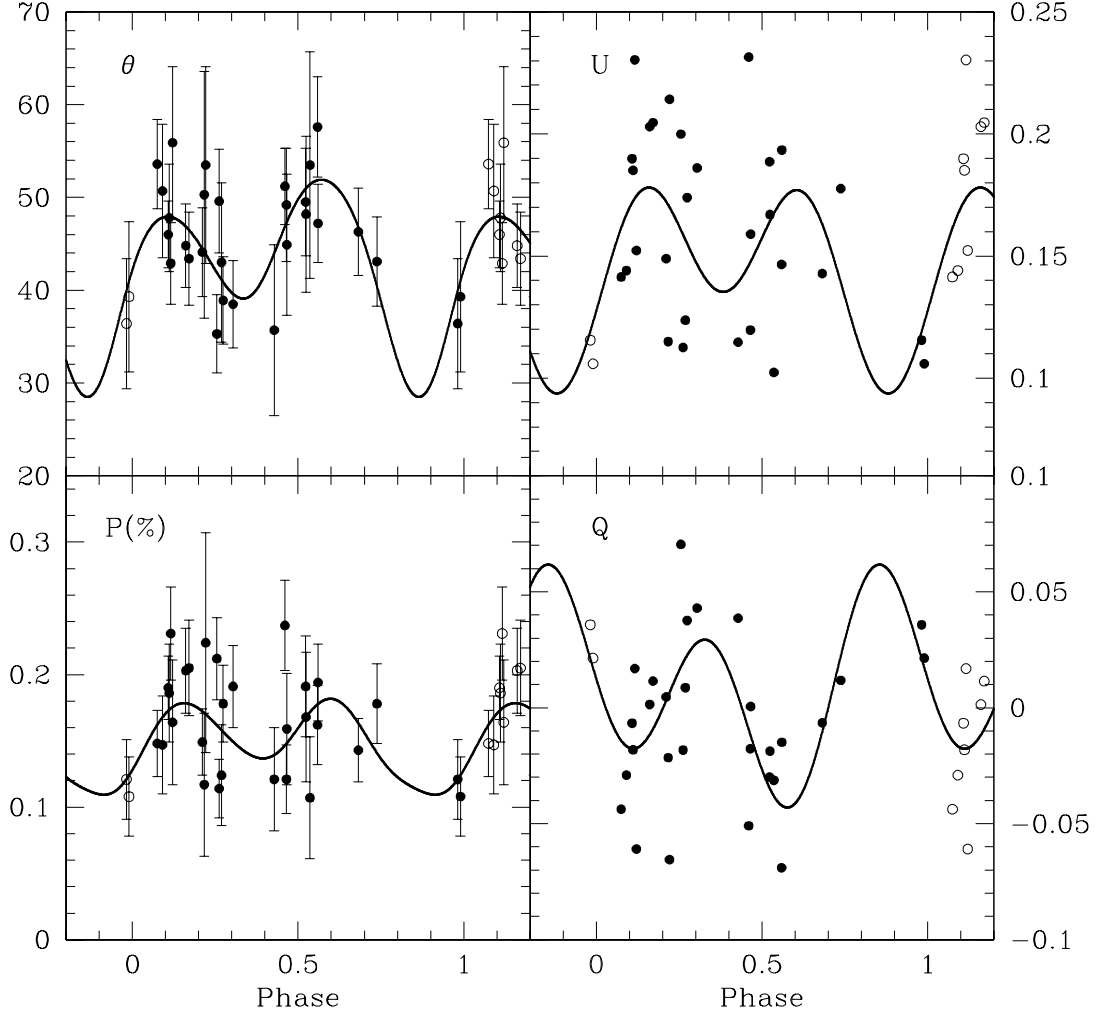


Fig. 15.— Polarimetric observations of Par 2494, which was determined to be constant in polarization. The first observation, taken in 1995 August, is not shown, since its polarization level and position angle are different from the rest of the data.

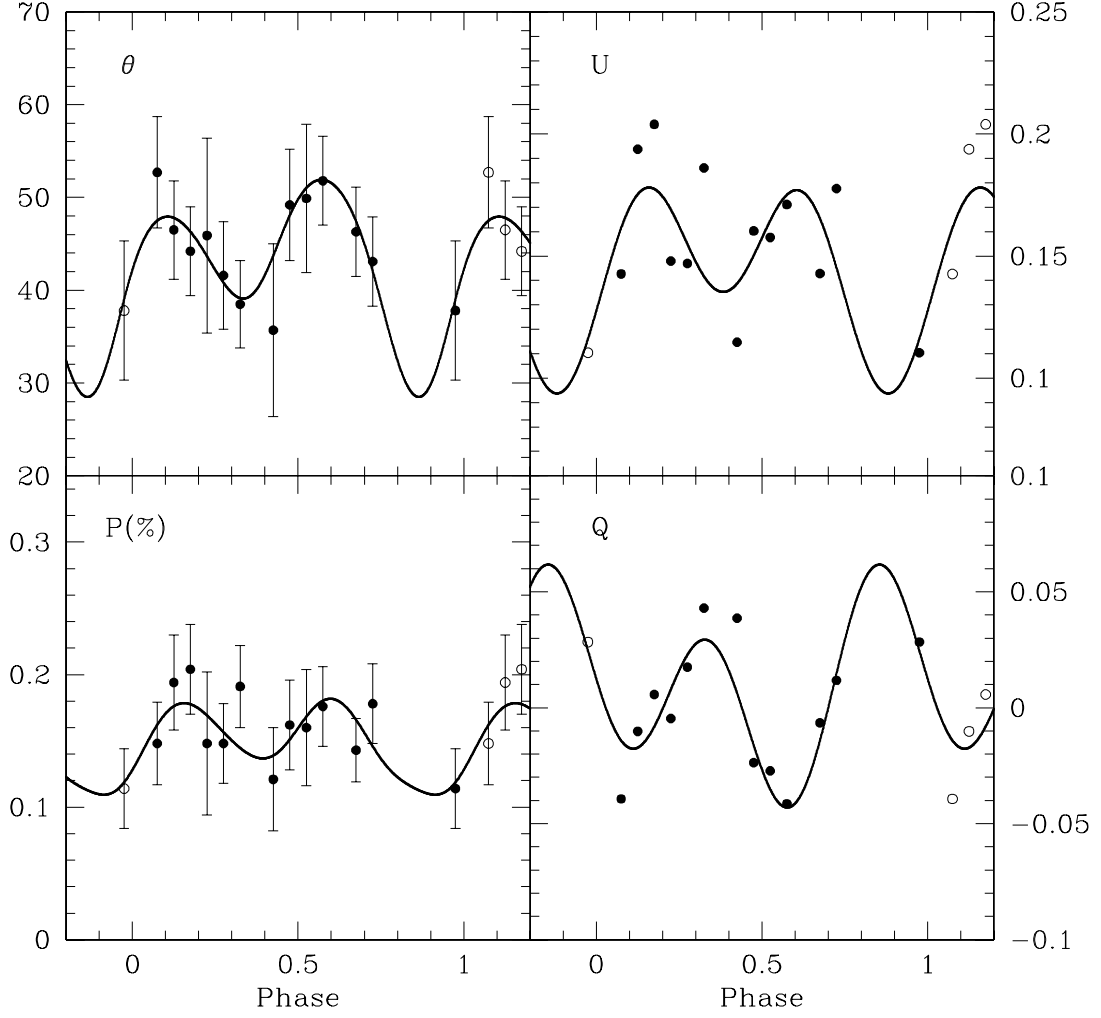


Fig. 16.— Binned data for polarimetric observations of Par 2494 reveal phased-locked variations in position angle.

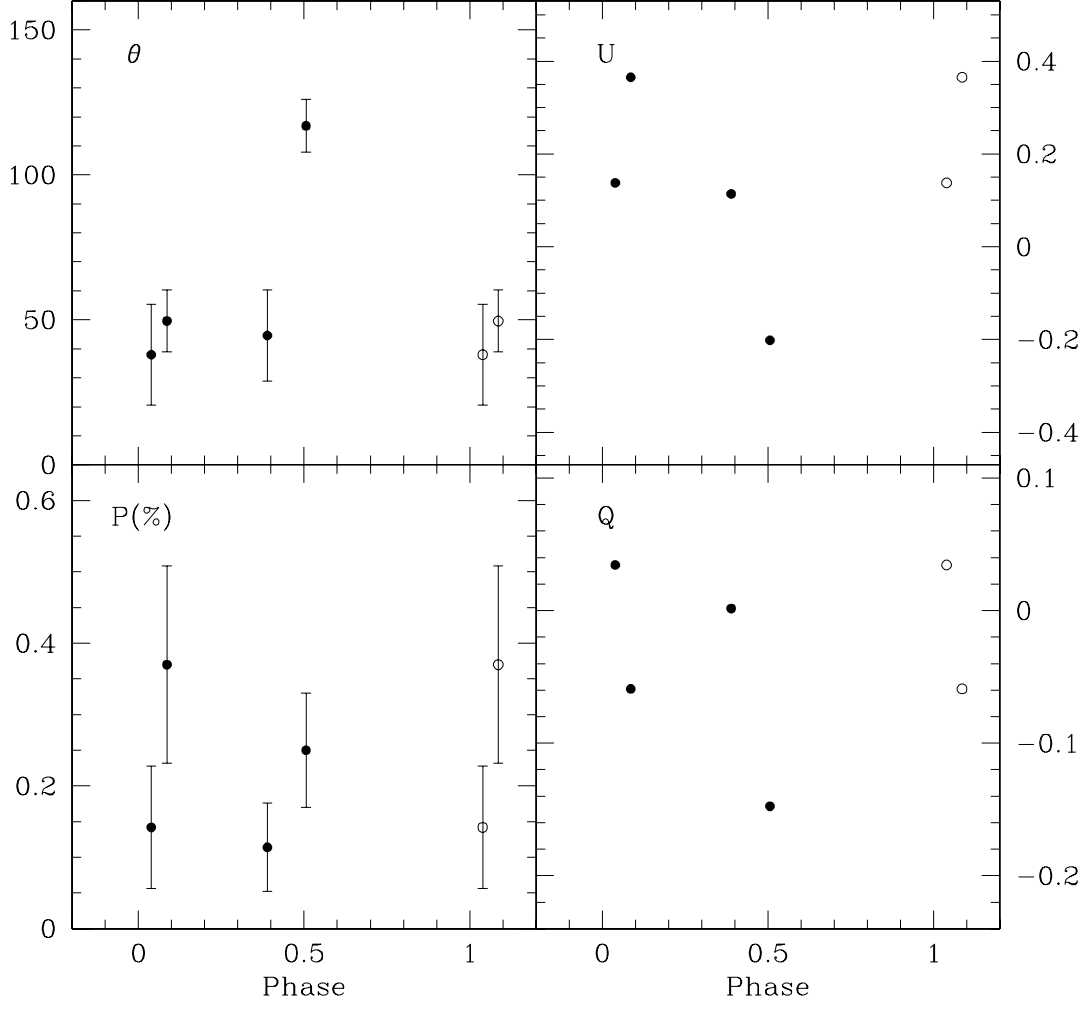


Fig. 17.— Polarimetric observations of Ori 569.

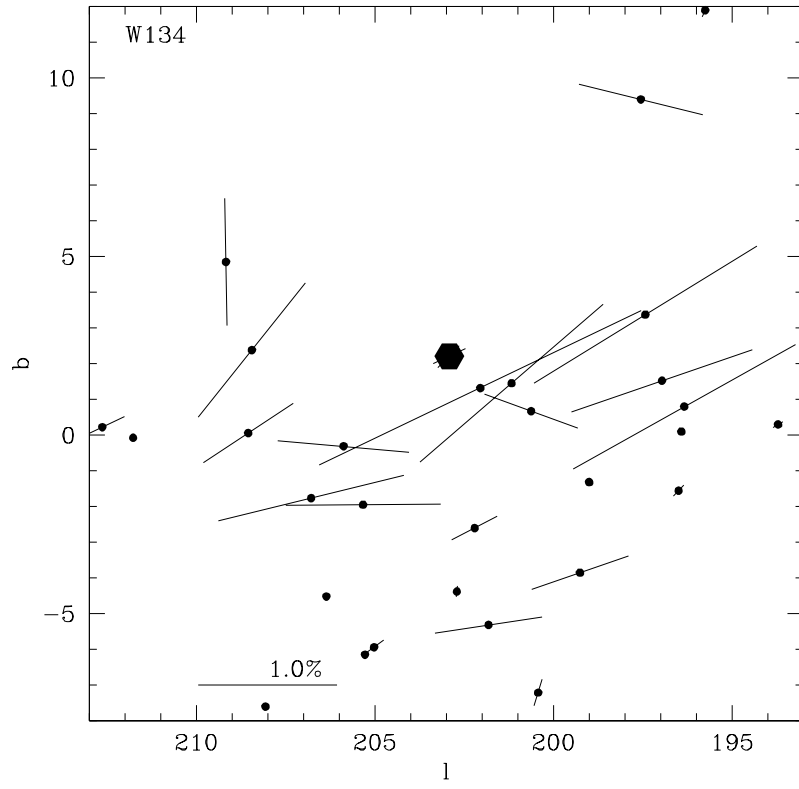


Fig. 18.— Map of the polarization in the vicinity of VSB 126 and W 134 (both at the center of the map). The stars selected to calculate the IS polarization are within 350 pc of those targets.

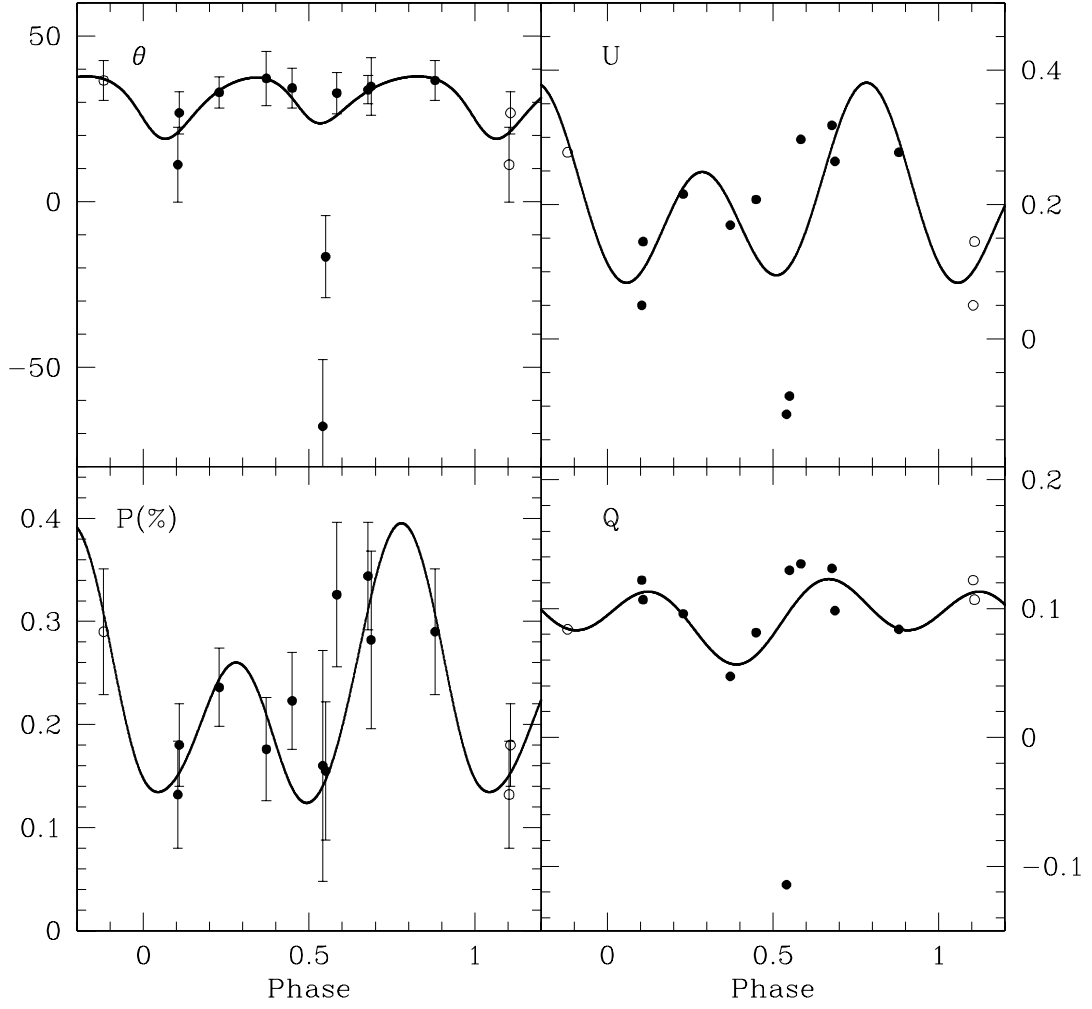


Fig. 19.— Polarimetric observations of W 134.

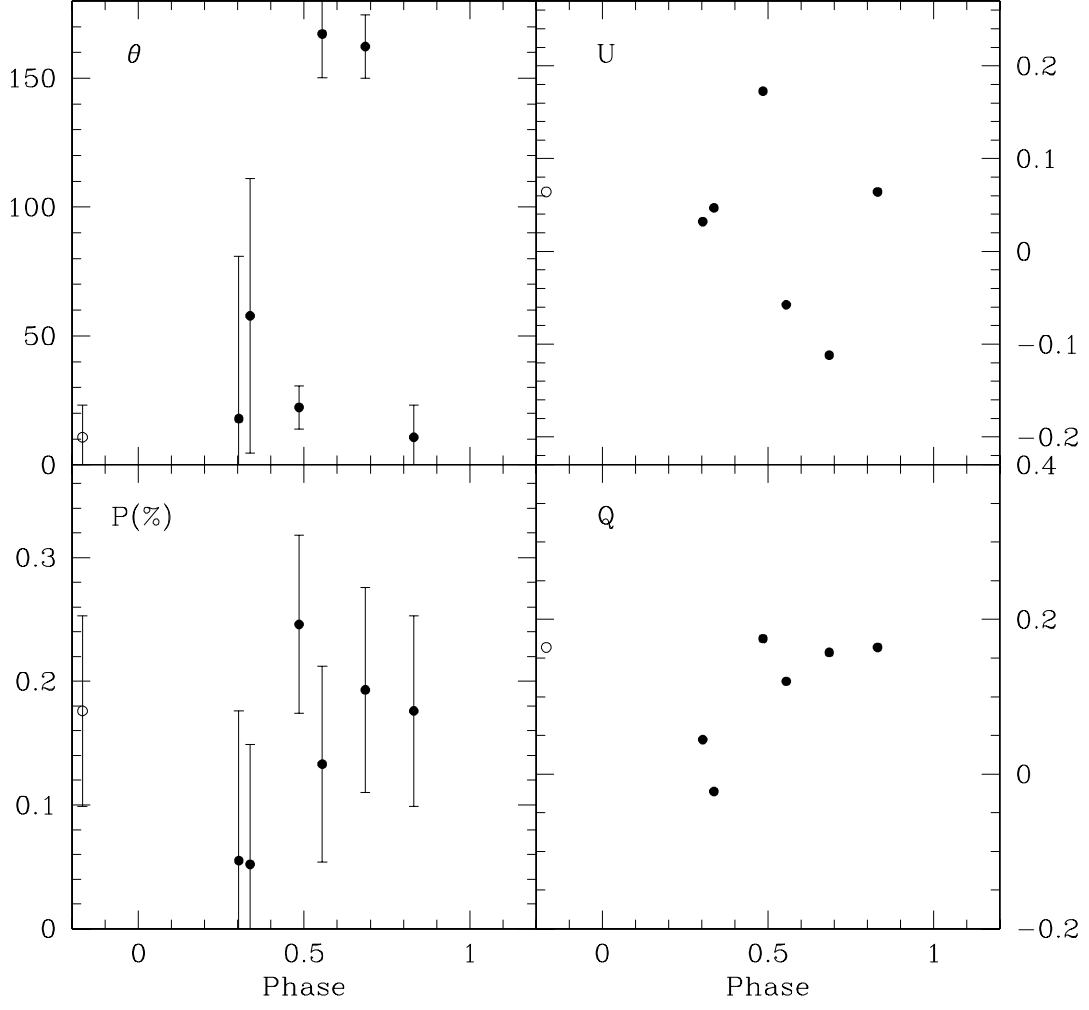


Fig. 20.— Polarimetric observations of VSB 126.

Table 1. Identification, coordinates, and location of the PMS binaries

Star	HBC ¹	Other Names	α^2 (2000.0)	δ^2 (2000.0)	Location
V773 Tau	367	HD 283447	04 14 13	+28 12 12	Tau-Aur L1495
LkCa 3	368	...	04 14 48	+27 52 35	Tau-Aur L1495
V826 Tau	400	TAP 43, FK 1	04 32 15	+18 01 42	Tau-Aur L1551
UZ Tau E/W	52	CoKu UZ Tau f	04 32 43	+25 52 31	Tau-Aur B217
DQ Tau	72	IRAS 04439+1654	04 46 52	+16 59 54	Tau-Aur L1558
NTTS 045251+3016	427	TAP 57, V397 Aur	04 56 02	+30 21 03	Tau-Aur L1517
GW Ori	85	HD 244138, BD +11 819	05 29 08	+11 52 13	λ Ori Assoc. B225
Par 1540	447	NGC 1977 334	05 34 41	−05 24 36	Trapezium
Par 2486	...	NGC 1977 1060, BD −05 1340	05 37 10	−05 10 36	Trapezium
Ori 429	05 34 41 ³	−02 33 54 ³	...
Par 2494	487	NGC 1977 1069, BD −06 1258	05 37 09	−06 06 12	Trapezium
Ori 569	05 44 29 ³	−00 10 30 ³	L1630 (M78)
W 134	536	NGC 2264 134, VAS 92, VSB 92	06 40 59	+09 55 20	NGC 2264
VSB 126	...	NGC 2264 169, NGC 2264 VAS 126	06 41 08	+09 44 03	NGC 2264

¹HBC numbers come from the Herbig and Bell Catalog (Herbig & Bell 1988).

²All coordinates except for Ori 429 and Ori 569 come from SIMBAD; coordinates for Ori 429 and Ori 569: F. Walter 1995, private communication.

³Equinox 1950.0 (F. Walter 1995, private communication).

Table 2. Spectroscopic and orbital information for the PMS binaries

Star ¹	Spectral Type	Ref.	Type ²	Ref.	sgl/ ³ dbl	Ref.	Period (d)	Ecc.	Ref.	Inc. (°)	Ref.	Dist. (pc)	Ref.
V773 Tau (3?)	K3 V(Li)	1	WT	1	dbl	2	51.075	0.267	2	$\gtrsim 66$	2	170	2
LkCa 3 (3)	M1 V(Li)	1	sgl	2	12.941	0.20	3	140	2
V826 Tau (2)	K5-K7 + K5-K7	4	WT	1	dbl	2	3.88776	0.0	3	7-13	5, 6	160	2
UZ Tau E (2)	M1,3:V(Li)	1	CT	1	sgl	7	19.1	0.28	7	140	...
DQ Tau	M0,1 V(Li)	1	CT	1	dbl	8	15.8	0.58	8
NTTS 045251+3016	K7(Li)	1	WT	1	sgl	9	2530	0.48	3
GW Ori (3)	G5 (Li)	1	CT	1	sgl	10	241.9	0.04	3	15-90	...	400	10
Par 1540 (2)	K4-K5	4	WT	4	dbl	11	33.73	0.12	3	470	12
Par 2486 (2)	dbl	3	5.1882	0.161	3	470	...
Ori 429 (2)	K3 + K3-K5	4	WT	4	dbl	4	7.46	0.27	3	470	4
Par 2494 (2)	K0 IV(Li)	1	dbl	...	19.4815	0.262	3	470	...
Ori 569 (3)	K4-K5 + K4-K5	4	WT	4	dbl	4	4.25	0.0	3	470	4
W 134 (2)	G5 V	1	dbl	...	6.3532	<0.01	13	46, 63	13	700	...
VSB 126 (2)	sgl	3	12.924	0.18	3	700	...

¹The numbers in parenthesis after each object indicate the number of stars in each system.

²Type of PMS star: CT (classical TTS), WT (weak-line TTS)

³Single-line (sgl) or double-line (dbl) spectroscopic binary.

References. — (1) Herbig & Bell 1988 (HBC catalog) and references cited; (2) Welty 1995; (3) Mathieu 1994 and references cited; (4) Lee, Martín, & Mathieu 1994; (5) Reipurth et al. 1990; (6) Mundt et al. 1983; (8) Stassun et al. 1996; (7) Mathieu, Martín, & Maguzzu 1996; (9) Walter et al. 1988; (10) Mathieu, Adams, & Latham 1991; (11) Marshall & Mathieu 1988; (12) Jones & Walker 1988; (13) Padgett & Stapelfeldt 1994

Table 3. Average observed polarization, origin of the polarization, and estimate of the intrinsic polarization for the PMS binaries

Star	P_{ave}^1 (%)	θ_{ave}^1 ($^\circ$)	N_{obs}	Origin of Polarization ²	P_{IS}^3 (%)	$\sigma(P_{\text{IS}})$ (%)	θ_{IS}^3 ($^\circ$)	$\sigma(\theta_{\text{IS}})$ ($^\circ$)	N_{IS}	Radius ($^\circ$)	Distance (\pm pc)	P_\star^4 (%)	θ_\star^4 ($^\circ$)
V773 Tau	0.35	88	6	$\star + \text{IS?}$	0.07	0.08	72	36	24	15	85	0.3	92
LkCa 3	0.05	76	12	$\text{IS} + \star?$	0.11	0.07	8	18	23	15	70	0.15	91
V826 Tau	0.85	67	11	\star	0.04	0.05	131	32	32	15	80	0.9	66
UZ Tau E/W	0.80	16	2	$\star + \text{IS}$	0.11	0.05	17	14	26	15	70	0.7	15
DQ Tau	0.57	79	1	$\star + \text{IS?}$	0.11	0.07	85	17	19	12	80	0.5	78
NTTS 045251+3016	0.10	107	3	$\star + \text{IS}$	0.20	0.07	58	9	18	15	80	0.2	136
GW Ori	0.61	126	11	$\star + \text{IS?}$	0.04	0.04	41	30	30	10	200	0.65	126
Par 1540	0.83	77	19	$\star + \text{IS}$	0.30	0.05	64	5	28	1.0	235	0.6	84
Par 2486	0.14	63	6	$\text{IS} + \star$	0.38	0.06	73	5	32	1.0	235	0.25	169
Ori 429	0.24	72	5	IS	0.35	0.07	92	6	21	2	235	0.2	23
Par 2494	0.16	46	29	$\star + \text{IS}$	0.26	0.05	78	5	48	2	235	0.2	7
Ori 569	0.18	76	4	$\star + \text{IS}$	0.21	0.04	90	5	68	6	235	0.1	29
W 134	0.22	32	11	$\star + \text{IS}$	0.87	0.12	177	4	20	8	350	0.8	80
VSJ 126	0.16	66	6	$\star + \text{IS}$	0.86	0.12	177	4	20	8	350	1.0	84

¹Weighted averages of the observed P and θ . The averages do not include atypical observations.

²Probable origin of the polarization. A \star symbol indicates intrinsic polarization; IS stands for interstellar polarization. If IS comes before a \star symbol, the IS component of the polarization is probably stronger than the intrinsic one.

³Estimate of the IS polarization at the location of the PMS binary, based on a weighted average of the polarization of stars in the neighborhood and at similar distance to the targets. Data taken from the Heiles (2000) catalog.

⁴Intrinsic polarization obtained after subtracting the estimated IS polarization.

Table 4. Use of the variability tests

Variability Result	Variance and Z Tests	χ^2 Test
Variable	≥ 3 PR	≥ 3 PR
	≥ 3 PR	2 PR, for same Stokes parameter as Variance and Z tests
	Z_Q and Z_U PR	≥ 3 PR
	σ_Q and Z_Q PR	≥ 3 PR
	σ_U and Z_U PR	≥ 3 PR
Suspected Var.	≥ 3 PR	1 PR
Possibly Const.	≥ 3 PR	0 PR
Constant	1 or 2 PR for the σ test, none for the Z test	0 PR

Note. — This table indicates the number of positive results (PR) from the variability tests needed to reach the different variability classification.

Table 5. Amplitude of the polarimetric variations¹

Star	ΔP (%)	$\Delta\theta$ (°)	ΔQ (%)	ΔU (%)	N_{obs}
V773 Tau	0.28	14.8	0.26	0.20	6
LkCa 3	0.13	97.9	0.13	0.08	12
V826 Tau	0.17	11.6	0.23	0.27	11
UZ Tau E/W	0.49	46.1	1.15	0.54	2
NTTS 045251+3016	0.10	28.5	0.07	0.11	3
GW Ori	0.22	17.2	0.33	0.31	11
Par 1540	0.17	9.3	0.22	0.24	19
Par 2486	0.18	28.4	0.09	0.19	6
Ori 429	0.21	9.3	0.20	0.13	5
Par 2494	0.13	22.3	0.14	0.13	29
Ori 569	0.26	78.9	0.18	0.57	4
W 134	0.21	128.8	0.25	0.43	11
VSB 126	0.19	156.6	0.20	0.29	6

¹Difference between the minimum and maximum values of the polarization, excluding, in some cases, very atypical observations.

Table 6. Results of the variability tests

Star	N_{obs}		σ_{sample}	σ_{mean}	$Z \pm \sigma Z$	$P\chi^2$ 1σ	$P\chi^2$ 1.5σ
V773 Tau	6	Q	0.0912	0.0122	3.36 0.32	1.00	1.00
		U	0.0777	0.0122	2.60 0.32	1.00	0.97
LkCa 3	12	Q	0.0314	0.0090	0.95 0.21	0.45	0.04
		U	0.0277	0.0090	0.84 0.21	0.27	0.02
V826 Tau	11	Q	0.0659	0.0104	1.69 0.22	0.99	0.76
		U	0.0753	0.0104	2.05 0.22	1.00	0.95
UZ Tau E/W	2	Q	0.8147	0.0274	21.03 0.71	1.00	1.00
		U	0.3819	0.0274	9.86 0.71	1.00	1.00
NTTS 045251+3016	3	Q	0.0399	0.0281	0.68 0.50	0.29	0.14
		U	0.0573	0.0281	1.10 0.50	0.70	0.42
GW Ori	11	Q	0.1119	0.0077	4.47 0.22	1.00	1.00
		U	0.0901	0.0077	3.04 0.22	1.00	1.00
Par 1540	19	Q	0.0529	0.0078	1.34 0.17	0.98	0.28
		U	0.0564	0.0078	1.39 0.17	0.99	0.38
Par 2486	6	Q	0.0378	0.0136	0.99 0.32	0.58	0.18
		U	0.0694	0.0136	1.88 0.32	0.99	0.84
Ori 429	5	Q	0.0776	0.0242	1.27 0.35	0.83	0.42
		U	0.0506	0.0242	0.92 0.35	0.48	0.15
Par 2494	29	Q	0.0342	0.0059	1.01 0.13	0.56	0.01
		U	0.0386	0.0059	1.17 0.13	0.90	0.05
Ori 569	4	Q	0.0800	0.0407	1.01 0.41	0.61	0.28
		U	0.2331	0.0407	2.47 0.41	1.00	0.95
W 134	11	Q	0.0706	0.0162	0.81 0.22	0.18	0.01
		U	0.1483	0.0162	2.13 0.22	1.00	0.97
VSB 126	6	Q	0.0790	0.0345	0.88 0.32	0.40	0.10
		U	0.0994	0.0345	1.29 0.32	0.86	0.41

Table 7. Classification of the observed PMS binaries, according to their variability

Variability Classification	PMS Binary
Variable	V773 Tau (6), V826 Tau (11), GW Ori (11) Par 1540 ¹ (19), W 134 (11)
Suspected variable	Par 2486 (6), Ori 569 (4)
Constant	LkCa 3 (12), NTTS 045251+3016 (3), Ori 429 (5), Par 2494 ¹ (29), VSB 126 (6)

¹These stars were sometimes observed to have very different polarization and/or position angle values (well above or below the majority of the data points) so their variability is based on data excluding those very atypical values.

Note. — The number of observations used for the variability tests is indicated in parentheses.

Table 8. Polarization data for V773 Tau

UT Date	JD 2400000.0+	Phase ¹	P (%)	$\sigma(P)$ (%)	θ (°)	$\sigma(\theta)$ (°)
1998 Jan 22	50835.493	0.316	0.189	0.025	94.9	3.8
1998 Dec 14	51161.509	0.699	0.469	0.058	80.1	3.6
1999 Feb 6	51215.615	0.179	0.397	0.033	85.6	2.4
1999 Feb 9	51218.668	0.239	0.369	0.023	93.0	1.7
1999 Feb 15	51224.632	0.355	0.385	0.033	86.1	2.5
1999 Mar 10	51247.586	0.384	0.432	0.031	82.6	2.0

¹Calculated with the ephemeris $2449900.0 + 51.075E$ (period from Jensen & Mathieu 1997).

Table 9. Polarization data for LkCa 3

UT Date	JD 2400000.0+	Phase ¹	P (%)	$\sigma(P)$ (%)	θ (°)	$\sigma(\theta)$ (°)
1996 Jan 3	50085.630	0.344	0.031	0.043	119.4	38.9
1996 Jan 5	50087.506	0.489	0.065	0.034	68.3	15.0
1996 Jan 7	50089.576	0.649	0.050	0.029	39.8	16.5
1996 Aug 24	50319.767	0.436	0.000	0.038	137.7	57.3
1996 Aug 25	50320.779	0.515	0.043	0.025	91.6	16.7
1996 Sep 4	50330.745	0.285	0.129	0.034	78.1	7.6
1996 Sep 7	50333.708	0.514	0.050	0.031	69.6	17.8
1996 Oct 12	50368.676	0.216	0.040	0.024	69.2	17.0
1997 Feb 9	50488.511	0.476	0.045	0.028	101.3	18.1
1997 Feb 14	50493.594	0.869	0.036	0.031	98.1	24.8
1997 Oct 18	50739.896	0.901	0.059	0.032	73.9	15.4
1997 Oct 26	50747.784	0.511	0.054	0.048	67.6	25.6

¹Calculated with the ephemeris $2449900.0 + 12.941E$ (period from Mathieu 1994).

Table 10. Polarization data for V826 Tau

UT Date	JD 2400000.0+	Phase ¹	P (%)	$\sigma(P)$ (%)	θ (°)	$\sigma(\theta)$ (°)
1994 Sep 22	49709.744	0.147	0.739	0.039	73.2	1.5
1994 Dec 23	50084.583	0.562	0.772	0.041	61.6	1.5
1996 Jan 2	50089.529	0.835	0.911	0.032	66.8	1.0
1996 Aug 25	50320.846	0.334	0.878	0.027	64.8	1.0
1996 Sep 7	50333.730	0.648	0.899	0.042	67.3	1.3
1996 Oct 12	50368.696	0.641	0.824	0.028	66.5	1.0
1997 Feb 9	50488.679	0.503	0.871	0.035	68.3	1.2
1997 Feb 14	50493.557	0.758	0.849	0.036	66.3	1.2
1997 Sep 9	50700.770	0.057	0.877	0.032	66.9	1.0
1997 Oct 26	50747.754	0.142	0.748	0.050	67.3	1.9
1998 Jan 22	50835.468	0.703	0.867	0.035	69.4	1.2

¹Calculated with the ephemeris $2446840.004 + 3.887758E$ (Reipurth et al. 1990).

Table 11. Polarization data for GW Ori

UT Date	JD 2400000.0+	Phase ¹	P (%)	$\sigma(P)$ (%)	θ (°)	$\sigma(\theta)$ (°)
1996 Dec 12	50429.896	0.442	0.654	0.031	123.4	1.4
1997 Feb 14	50493.628	0.706	0.677	0.028	118.3	1.2
1997 Sep 9	50700.795	0.562	0.585	0.020	129.2	1.0
1997 Oct 26	50747.828	0.757	0.566	0.033	127.0	1.7
1997 Nov 4	50756.930	0.794	0.666	0.030	128.7	1.3
1998 Jan 23	50836.552	0.123	0.533	0.021	130.8	1.1
1998 Feb 16	50860.623	0.223	0.626	0.021	123.8	0.9
1998 Aug 28	51053.800	0.021	0.639	0.023	124.7	1.0
1999 Feb 9	51218.711	0.703	0.569	0.026	114.4	1.3
1999 Feb 15	51224.668	0.810	0.616	0.030	114.6	1.4
1999 Mar 9	51246.607	0.818	0.460	0.034	113.6	2.1

¹Calculated with the ephemeris $2445001 + 241.9E$ (Mathieu et al. 1991).

Table 12. Polarization data for Par 1540

UT Date	JD 2400000.0+	Phase ¹	P (%)	$\sigma(P)$ (%)	θ (°)	$\sigma(\theta)$ (°)
1996 Jan 7	50089.667	0.696	1.072	0.055	82.1	1.5
1996 Oct 12	50368.755	0.970	0.907	0.071	82.5	2.3
1997 Feb 9	50488.541	0.521	0.753	0.026	77.1	1.0
1997 Feb 14	50493.533	0.669	0.855	0.032	75.7	1.1
1997 Sep 8	50699.867	0.787	0.807	0.048	73.2	1.7
1997 Oct 18	50739.848	0.972	0.810	0.031	76.0	1.1
1997 Oct 25	50746.770	0.177	0.793	0.038	78.1	1.4
1997 Oct 26	50747.858	0.209	0.855	0.046	74.6	1.5
1997 Nov 4	50756.895	0.477	0.826	0.036	76.8	1.3
1998 Jan 13	50826.593	0.544	0.765	0.024	77.9	0.9
1998 Jan 23	50836.570	0.839	0.845	0.030	78.1	1.0
1998 Feb 15	50859.587	0.522	0.813	0.031	77.1	1.1
1998 Feb 16	50860.556	0.551	0.882	0.029	77.7	0.9
1998 Dec 10	51157.704	0.360	0.918	0.038	74.5	1.2
1999 Feb 4	51213.627	0.018	0.748	0.046	75.9	1.8
1999 Feb 6	51215.555	0.075	0.874	0.045	78.2	1.5
1999 Feb 9	51218.618	0.166	0.888	0.028	76.4	0.9
1999 Feb 14	51223.561	0.313	0.863	0.036	76.2	1.2
1999 Feb 15	51224.598	0.343	0.842	0.032	74.7	1.1
1999 Mar 9	51246.542	0.994	0.795	0.048	77.6	1.7

¹Calculated with the ephemeris $2444972.95 + 33.73E$ (Marschall & Mathieu 1988).

Table 13. Polarization data for Par 2486

UT Date	JD 2400000.0+	Phase ¹	P (%)	$\sigma(P)$ (%)	θ (°)	$\sigma(\theta)$ (°)
1995 Dec 14	50065.738	0.945	0.125	0.023	63.8	5.2
1996 Oct 12	50368.779	0.354	0.097	0.039	59.7	11.6
1997 Feb 9	50488.625	0.454	0.117	0.038	85.8	9.2
1997 Oct 19	50740.863	0.072	0.055	0.039	57.4	20.7
1998 Jan 23	50836.613	0.527	0.190	0.036	63.2	5.5
1998 Feb 16	50860.641	0.158	0.232	0.036	58.1	4.5

¹Calculated with the ephemeris $2449900.0 + 5.1882E$ (period from Mathieu 1994).

Table 14. Polarization data for Ori 429

UT Date	JD 2400000.0+	Phase ¹	P (%)	$\sigma(P)$ (%)	θ (°)	$\sigma(\theta)$ (°)
1995 Dec 14	50065.689	0.210	0.268	0.043	69.0	4.6
1996 Jan 7	50089.617	0.417	0.293	0.066	78.3	6.5
1996 Jan 7	50089.643	0.421	0.085	0.061	70.4	20.6
1996 Oct 12	50368.723	0.831	0.290	0.053	72.7	5.2
1997 Feb 9	50488.595	0.900	0.242	0.057	69.9	6.7

¹Calculated with the ephemeris $2449900.0 + 7.460E$ (period from Mathieu 1994).

Table 15. Polarization data for Par 2494

UT Date	JD 2400000.0+	Phase ¹	P (%)	$\sigma(P)$ (%)	θ (°)	$\sigma(\theta)$ (°)
1995 Aug 28	49957.860	0.969	0.352	0.030	27.8	2.4
1995 Sep 3	49963.800	0.274	0.178	0.029	38.9	4.7
1996 Jan 7	50089.715	0.738	0.178	0.030	43.1	4.8
1996 Sep 4	50330.868	0.116	0.231	0.035	42.9	4.4
1996 Sep 7	50333.844	0.269	0.124	0.038	43.0	8.6
1997 Jan 1	50449.724	0.217	0.117	0.054	50.3	13.3
1997 Feb 9	50488.569	0.211	0.149	0.025	44.1	4.8
1997 Feb 10	50489.566	0.262	0.114	0.022	49.6	5.6
1997 Feb 14	50493.508	0.465	0.121	0.026	49.2	6.1
1997 Sep 9	50700.859	0.108	0.190	0.024	46.0	3.6
1997 Oct 18	50739.870	0.111	0.186	0.037	47.8	5.8
1997 Oct 19	50740.844	0.161	0.203	0.032	44.8	4.5
1997 Oct 25	50746.797	0.466	0.159	0.042	44.9	7.6
1997 Oct 26	50747.894	0.523	0.191	0.038	49.5	5.8
1997 Nov 4	50756.847	0.982	0.121	0.030	36.4	7.0
1998 Jan 13	50826.546	0.560	0.194	0.029	47.2	4.2
1998 Jan 23	50836.592	0.075	0.148	0.025	53.6	4.8
1998 Feb 15	50859.562	0.255	0.212	0.031	35.3	4.2
1998 Feb 16	50860.527	0.304	0.191	0.031	38.5	4.7
1998 Nov 14	51131.644	0.221	0.224	0.083	53.5	10.6
1998 Dec 8	51155.797	0.460	0.237	0.034	51.2	4.1
1998 Dec 10	51157.725	0.559	0.162	0.030	57.6	5.4
1998 Dec 29	51176.758	0.536	0.107	0.046	53.5	12.2
1999 Feb 4	51213.604	0.428	0.121	0.039	35.7	9.2
1999 Feb 5	51215.484	0.524	0.168	0.049	48.2	8.4
1999 Feb 9	51218.558	0.682	0.143	0.024	46.3	4.7
1999 Feb 15	51224.548	0.990	0.108	0.030	39.3	8.1
1999 Feb 17	51226.518	0.091	0.147	0.037	50.7	7.2
1999 Mar 9	51246.588	0.121	0.164	0.047	55.9	8.2
1999 Mar 10	51247.557	0.171	0.205	0.036	43.4	5.0

¹Calculated with the ephemeris $2449900.0 + 19.4815E$ (period from Mathieu 1994).

Table 16. Polarization data for W 134

UT Date	JD 2400000.0+	Phase ¹	P (%)	$\sigma(P)$ (%)	θ (°)	$\sigma(\theta)$ (°)
1995 Dec 14	50065.781	0.108	0.180	0.040	26.8	6.4
1996 Jan 2	50084.813	0.104	0.132	0.052	11.2	11.3
1996 Jan 7	50089.745	0.880	0.290	0.061	36.6	6.0
1997 Jan 1	50449.783	0.550	0.155	0.067	-16.6	12.4
1997 Feb 9	50488.711	0.678	0.344	0.052	33.8	4.3
1997 Oct 19	50740.892	0.371	0.176	0.050	37.2	8.2
1998 Jan 23	50836.685	0.449	0.223	0.047	34.3	6.0
1998 Feb 16	50860.699	0.229	0.236	0.038	33.0	4.7
1998 Apr 29	50932.567	0.541	0.160	0.112	112.2	20.1
1999 Feb 9	51218.734	0.584	0.326	0.070	32.8	6.2
1999 Feb 16	51225.742	0.687	0.282	0.086	34.8	8.7

¹Calculated with the ephemeris $2447472.985 + 6.3532E$ (Padgett & Stapelfeldt 1994).

Table 17. Polarization data for VSB 126

UT Date	JD 2400000.0+	Phase ¹	P (%)	$\sigma(P)$ (%)	θ (°)	$\sigma(\theta)$ (°)
1995 Dec 14	50065.828	0.831	0.176	0.077	10.7	12.5
1996 Jan 2	50084.861	0.303	0.055	0.121	17.9	63.0
1996 Jan 7	50089.795	0.685	0.193	0.083	162.3	12.3
1997 Feb 9	50488.758	0.555	0.133	0.079	167.2	17.0
1998 Jan 23	50836.803	0.485	0.246	0.072	22.3	8.4
1998 Feb 16	50860.734	0.337	0.052	0.097	57.8	53.3

¹Calculated with the ephemeris $2449900.0 + 12.9240E$ (period from Mathieu 1994).

Table 18. Polarization data for other stars

Star	UT Date	JD 2400000.0+	Phase	P (%)	$\sigma(P)$ (%)	θ ($^\circ$)	$\sigma(\theta)$ ($^\circ$)
UZ Tau E/W	1997 Sep 9	50700.684	0.920 ¹	0.604	0.035	47.7	1.6
UZ Tau E/W	1998 Jan 23	50836.514	0.032	1.097	0.044	1.6	1.1
DQ Tau	1997 Sep 9	50700.745	0.753 ²	0.571	0.048	78.9	2.4
NTTS 045251+3016	1997 Jan 1	50449.687	0.217 ³	0.026	0.076	90.9	57.7
NTTS 045251+3016	1997 Oct 26	50747.807	0.335	0.125	0.050	119.4	11.3
NTTS 045251+3016	1998 Jan 23	50836.535	0.370	0.095	0.038	95.0	11.4
Ori 569	1996 Sep 7	50333.866	0.086 ⁴	0.370	0.138	49.6	10.7
Ori 569	1997 Feb 9	50488.653	0.506	0.250	0.080	116.9	9.1
Ori 569	1998 Jan 23	50836.654	0.389	0.114	0.062	44.6	15.8
Ori 569	1998 Feb 16	50860.667	0.039	0.142	0.086	38.0	17.4

¹Calculated with the ephemeris $2449900.0 + 19.1E$ (period from Mathieu et al. 1996).

²Calculated with the ephemeris $2449582.54 + 15.8043E$ (Mathieu et al. 1997).

³Calculated with the ephemeris $2449900.0 + 2530E$ (Mathieu 1994).

⁴Calculated with the ephemeris $2449900.0 + 4.25E$ (Mathieu 1994).

Table 19. Noise analysis and orbital inclination from the BME formalism for some observed binaries

Star	DQ	γ	Noise ¹ for Q	Noise for U	$i(\mathcal{O}2)$ ($^{\circ}$)	$\sigma(i(\mathcal{O}2))$ ($^{\circ}$)	$i(\mathcal{O}1)$ ($^{\circ}$)	$\sigma(i(\mathcal{O}1))$ ($^{\circ}$)
LkCa 3	0.346	4.2	0.25	0.35	93.9	25.4	72.3	65.5
V826 Tau	0.165	18.3	0.30	0.23	92.7	5.3	25.3	57.7
GW Ori	0.109	42.2	0.36	0.28	79.7	6.3	107.6	15.7
Par 1540	0.242	8.5	0.22	0.17	96.4	6.5	117.5	38.5
Par 2494	0.140	25.5	0.19	0.28	97.3	7.0	77.0	22.9
W 134	0.203	12.1	0.18	0.25	83.9	7.0	95.0	22.5

¹The noise is the square root of the variance of the fit over the amplitude of the variations; the amplitude comes from the maximum values of the data and not of the fit.

Table 20. Other parameters returned by the BME formalism: Ω , the orientation of the orbital plane, and moments of the distribution of the scatterers.

Star	Ω ($^\circ$)	$\sigma(\Omega)$ ($^\circ$)	$\tau_0 G$ $\times 10^{-4}$	$\tau_0 H$ $\times 10^{-4}$	$\tau_0 G / \tau_0 H$
LkCa 3	58.0	48.1	1.20	2.59	2.16
V826 Tau	96.4	12.6	4.35	7.32	1.68
GW Ori	171.9	12.9	2.63	6.71	2.56
Par 1540	109.6	7.3	0.98	3.96	4.02
Par 2494	141.3	16.3	1.47	4.60	3.14
W 134	91.9	14.7	3.41	10.9	3.20